Comparison of Three Single-passage SAHs with Different Modifications

Shadi Ayyad

Submitted to the
Institute of Graduate Studies and Research
in partial fulfillment of the requirements for the Degree of

Master of Science
in
Mechanical Engineering

Eastern Mediterranean University
September 2013
Gazimağusa, North Cypru

Approval of the Institute of Graduate Studies and Research

Prof. Dr. Elvan Yılmaz
Director

I certify that this thesis satisfies the requirements as a thesis for the degree of Master of Science in Mechanical Engineering.

Prof. Dr. Uğur Atikol
Chair, Department of Mechanical Engineering

We certify that we have read this thesis and that in our opinion it is fully adequate in scope and quality as a thesis for the degree of Master of Science in Mechanical Engineering.

Prof. Dr. Fuat Egelioğlu
Co-Supervisor

Assoc.Prof.Dr.Hasan Hacışevki
Supervisor

ExaminingCommittee

1. Prof. Dr. Uğur Atikol

3. Assoc. Prof. Dr. Hasan Hacışevki

2. Assoc. Prof. Dr. Serkan Abassoğlu

ABSTRACT

The increasing costs of fossil fuels and the influence of their harmful combustion products on the climate change, which has dramatically been revealed in this century are considered as critical dynamics behind the global search for different suggestions to meet these urgent challenges. In the present work, three different types of solar air heaters (SAHs). One of the collector consist of fins attached to aluminum plate and the other collectors made of two different sizes of aluminum square tubes as absorber plates were experimentally investigated in order to achieve the most efficient design of the proposed SAHs. Experiments were conducted, based on the ASHRAE standards, under Famagusta - Cyprus climatic conditions. The thermal performances of the three collectors were examined over a broad range of operating and design conditions. Results showed that there was no superiority for one collector over the other. The effect of mass flow rate on the performance was different for each SAH. At low mass flow rates it was found that the SAH having 20 x 20 mm square aluminum tubes as absorber plate has the highest efficiency which was calculated as 86%; whereas, the maximum efficiency at higher mass flow rates was obtained in the SAH having finned absorber plate which was 93%.

Key words: Solar air heater, Thermal efficiency, Collectors, Temperature, Panels.

ÖZ

Fosil yakıtların fiyatlarındaki artış ve yanma sonucu ortaya çıkan zaralı bileşiklerin iklim değişikliği üzerindeki etkileri global olarak başka acil çözümler aranması üzerinde önemli dinamikler teşkil etmektedir. Bu çalışmada üç değişik tipte Havalı Güneş Isıtıcıları (HGI) finli düz ve iki değişik ölçüde kare alüminyum profiller emici yüzey olarak en verimli tasarımı belirlemek için deneylerde kullanılmışlardır. Deneyler Kıbrıs – Mağusa koşulları altında, ASHRAE standartlarına göre yürütülmüştür. Kollektörlerin ısıl performansları geniş bir işletme ve tasarım aralığı üzerinde incelenmiştir. Sonuçlar her üç tipin de birbiri üzerine büyük bir üstünlük sağlamadığını göstermiştir. Hava akış oranının her bir tasarım üzerindeki etkisi farklı olmuştur. Düşük hava akış oranlarında 20 x 20 mm ölçüsündeki aluminyum kollektörün %86'lık en yüksek verimi verdiği hesaplanmıştır. En yüksek verim ise fin tipi emici plakası olan kollektör tarafından %93 olarak yüksek hava akış oranlarında elde edilmiştir.

Anahtar kelimeler: Güneş hava ısıtıcı, Isıl verim, Collectors, paneller, Sıcaklık

To My Family

ACKNOWLEDGMENT

I would like to thank my respect supervisor Assoc. Prof. Dr. Hasan Hacışevki., who has stood with me in this thesis and I am greatly thankful to my dear professor for all his advices, guidance, continuous help and valuable support.

I'd like also to send my thanks and best regards for Prof. Dr. Fuat Egelioğlu who suggested me to write in this area and for his valuable advices. I am also obliged for Assist. Maher Ghazal for his ongoing support during my study and research.

Really I would not ignore all my dear professors and instructors who have taught me in this university, which really I have learned many valuable things and spent special times with many friends from the all distinct nationalities. Special thanks for technical staff in my department Mr. Zafer Mulla and Mr. Servet Uyanık.

My message of respect and appreciation to my friends Motaz, Ahmad, Ashraf, Ammar, and Ali and also the friends from the other different nationalities.

I would like to say something for my beloved friends in Palestine, Gaza Strip for their ongoing support and I promise you that these moments will not be forgotten.

TABLE OF CONTENTS

LIST OF FIGURES

LIST OF SYMBOLS

A_c	Area of collector, m^2
C_p	Specific heat of the fluid (kJ/kg. K)
I	Solar radiation (W/m2)
$\dot{m}$	Mass flow rate (kg/s)
Q	Volumetric flow rate (m^3/s)
V	Velocity of the outlet air(m/s)
T_{in}	Inlet temperature (^OC)
T_{out}	Outlet temperature (^OC)
ΔT	Temperature difference (^OC)
η	Thermal efficiency of solar collector
q	Density of air (kg/m3)
ω_m	Uncertainty for mass flow rate
ω_η	Uncertainty for thermal efficiency

Chapter 1

INTRODUCTION

Solar air heater is a mechanism that leads to an increase in the temperature of the air by absorbing radiation from the sun. At present, SAHs are widely used in several places in agriculture, space heating, industry, etc. These devices are among the most efficient ways of minimizing the cost of heating. SAHs can be used in processing applications such as drying agricultural products (i.e. tea, corn, coffee) and other drying applications. Air is heated through a solar device and then directed over a medium to be dried; hence this mechanism provides an efficient way to reduce the moist content of products [1]. SAHs can be applied as ancillary heaters to heat buildings to reduce the cost of energy. The gradual depletion of petroleum supplies and the uncertainty of its cost have increased the concern of the people. Burning fossil fuels emits hazardous products such as CO_2, CO, SO_x, NO_x, etc. CO_2 is a greenhouse gas, SOx and NOx are responsible for acid rain precipitation. Moreover, the poisonous gases such as CO which is produced by combustion of fuels causes damages to human health. These fears have forced the researchers to find new environmentally friendly sources of energy such as solar energy to catch-up the societies' growing energy demands and save classical energy. The sun has been the most powerful heat generator since the beginning of the life.

Nowadays, the major achievements in technology in many fields of engineering and science make it achievable to produce the potential solar energy that satisfies the world's requirements in the field of energy [2].

SAHs have been mentioned as the most powerful energy suppliers in buildings in an environmentally friendly energy field; in addition, CO_2 emissions recorded the lowest amount compared with other energy sources. In spite of the successes of solar air systems, these heaters are still limited in use around the world. The poor financial conditions make the scientists develop reliable and cheap solar air heating systems [3].

North Cyprus is one of the leading countries where solar water heating systems are widely used. In North Cyprus the usage of SAHs is almost none. The main aim of this study is to construct three different SAHs and experimentally investigate their performance under the climatic conditions of North Cyprus.

Chapter 2

LITERATURE REVIEW

The history of solar energy assortment dates back to 1776, when a Swiss man called DeSaussure [4] discovered a simple collector generally referred to as a 'Hot box'. SAHs are comprised of three primary parts which are panels, encased hot air channels, and air blowers. The components of the panel are an absorber plate and a transparent cover (i.e., glazing).The solar radiation passes through the glazing and is absorbed by the absorber plate; then, the air flowing over the absorber plate gains heat by convection.

The major heat is lost through the glazing. Heat losses from the sides and bottom of the collector are low as the sides and bottom are insulated. The transferring heat coefficient between the air and the absorber plate is low. The temperature of the absorber plate increases because of the incoming solar radiation. As the absorber plate's temperature increases, radiation losses also increase. Low thermal efficiencies are achieved in old air heaters (i.e., flat plate SAHs). In order to maximize thermal efficiency, many modifications and configurations of absorber plates are suggested. Solar air heaters are developed with totally different shapes of the flowing air paths inside the solar panels [5]. Several modifications were made; for example, linear fins were attached to the absorber plate [6], or corrugated absorber plate [7], hollow spheres [8], and solid matrix [9] were added to the construct. Various factors such as length and depth of the collector, type of cover

plate, speed of the air, type of absorber plate, etc affect the efficiency of solar collectors. Shape of the absorber plate can be considered as the most important factor.

The increase of the size of the absorber plate within the collector will cause a rise in the heat transferred to the flowing air. Although thermal efficiency increases, pressure drop also increases; thus, to pump the air inside the panel extra energy is required [10].

As mentioned before, one of the main problems which affects the efficiency of the collector is the heat lost through the cover plate. Several realizations have been done in order to maximize thermal performance by minimizing the heat loss through the transparent cover. Using double glazing is one of the main recommendations [11, 12]. In double pass structures, air enters through the upper transparent plate and then turns over to pass through the lower transparent plate which functions as a second glass [13, 14] or vice versa [l5, 16]. Researchers such as Esen [17], and Ozgen et al. [18] conducted a study and recommended entrance of the air from the top and beneath the absorber plate in a multi flow stream of SAH. In the same vein, Yeh et al. [19, 20] proposed that we can obtain a higher thermal efficiency by using a multi pass solar air heater where the cross-section areas of lower and upper flow streams are structured equally, and at the time when the rates of the mass flow in both flow streams are equal. In another research, Jain and Jain [21] checked double pass channels of a SAH and presented what they achieved. Moreover, Mohammad [22] introduced and analyzed the counter flow solar air heater for multi pass channels with many porous media in the underneath channel.

Paisarn [23] analyzed multi pass SAHs with linearly attached fins .Bliss [24] used packing absorbent materials to absorb the sun radiation in solar panels.

Many researchers used several cheap materials to find out the suitability of using these heaters within the developing countries. For example, stone [25] and iron turnings [26] are used in the collector to improve the efficiency. Also another studied conducted to investigate the performance of different materials as absorber plates like using metal wool [27], crushed glass [28] , stone and wool [29], plants [30] work on the same idea. Black oxidized and black galvanized metal wire screens [31] are some other materials used to improve the performance of SAHs.

Many researchers tried to maximize the thermal efficiency of SAHs by employing packing bed inside the duct of solar collector via using cross rod matrices and slit-and-aluminum-foil matrices. For example, Ramadan et al., [32], Tong and London [33], Sopian et al. [34], Hasatani et al. [35], Beckman [36], Harnid and Beckman [37], Chiou et al. [38], Thakur et al. [39], Ozturk and Dernirel [40], Kays and London [41], Choudahary and Garg [42], Varshney and Saini [43], Mittal and Varsluiey [44], and Coppage and London [45] used packing bed materials to increase the efficiency of SAHs.

Varshney and Saini [46] have experimentally investigated the characteristics of a solar air collector and the heat transfer of fluid flow by using wire mesh packed screen matrices in its duct where air is flowing parallel to matrix planes. Sopian et al. [47] inspected the performance of multi pass SAH collectors with porous media in lower or upper stream. The rate of transferred heat and the properties of

the fluid flow of solar heater using wire mesh packing with a range of porosity of 0.667-0.880 have been experimentally investigated by Thakur et al. [48]. Researchers have found out that the volumetric heat transfer coefficient is inversely proportional with porosity. Therefore, minimum porosity can be a good option as far as thermal performance is concerned in SAHs.

The thermal effectiveness of a solar air collector using 'Raschig' circle within the flow stream packed has been experimentally investigated by Ozturk and Demirel [49]. In addition, Mittal and Varshney [50] have scrutinized the thermal efficacy of a SAH packing bed using wire mesh matrices for various geometric parameters. The transferred heat rate and the air mass flow rate characteristics of a solar air collector packed bed with wire mesh screen matrices have been inspected and compared with conventional SAHs by Prasad et al. [51].

The aim of using transpired solar air heaters is to minimize the energy consumption and operating costs that are related to bracing air ventilation demands. The ambient air is heated by entering inside the transpired solar collector through tiny gaps on black dyed surface that is heated by solar rays. Commonly, it is installed south oriented and located in a place to receive the maximum amount of sunlight. Transpired collectors use sun radiation to reheat ambient air as it is entered into premises. It should be noted that, transpired solar air heaters do not have glazing. It is estimated that every square foot of a transpired collector increases the temperature of a 4 cubic feet per meter (cfm) by the degree of 40°F, and transmits an amount of heat by 240,000 Btu per square foot of the solar air heater panel [52-53]. The angle and the height of the sun radiation change every week during the

year. The amount of observed sun radiation mainly depends on the angle of the collectors over a year. The highest amount of solar radiation which can be consumed by the collector is during summer season and the lowest amount of radiation consumed is in the winter. In order to achieve greatest efficiency of the collectors, the sun radiations should be used thoroughly through the whole year. The solar air heater collectors should be installed vertically or horizontally facing the south side of the building on the roof in order to consume the maximum amount of sun radiation [54].

2.1 The Objective of the present study

The main objective of this study is to investigate experimentally the thermal performance of the three different types of SAHs, and then to compare the results with the other studies available in the literature. Therefore, three SAHs were constructed, with single air passages comprised of different absorber plates. The first one has an absorber plate made of square aluminium tubes with cross-sectional dimensions of 20 x 20 mm, and wall thickness of 2 mm. The second one is composed of an absorber plate made of square aluminium tubes with dimensions of 25 x 25 mm and wall thickness of 2 mm. The third SAH consists of fins attached to an aluminium plate as an absorber plate. The length of the absorber plates are 1540 mm.

Chapter 3

EXPERIMANTAL WORK

3.1Apparatus

The three SAHs are constructed with casings having dimensions of 1930 mm length, 960 mm width and120 mm depth. The pictorial views of the SAHs are presented in Fig. 1. In which the attached fins can be clearly seen. Sectional views of the tube type panels are presented in Figs. 3.2. Figure. 3.3 shows the sectional view of fin type collector.

Figure 3.1: Solar air heater collectors.

The panels and the tubes are painted in black color in order to increase the absorption of heat from the sun radiation. All the panels have been insulated from the bottom by deploying a wood board of 1540mm length, 910mm width and 15mm thickness. Moreover, to serve the purpose of insulation, expanded polystyrene with a thickness of 20mm was placed at the bottom. To reduce the heat loss from the sides, the inner and outer surfaces were insulated by expanded polystyrene. In order to allow air inlet and outlet through the panel, a wooden box was designed and installed at the lower and upper parts of the panel, respectively.

An induced draft fan was placed at the upper side (i.e., outlet section) of each panel to suck air from the lower bottom, pass it through the panel and blow it out. To control the speed of the fan (i.e., the air mass flow rate) dimmer switches were employed. Three plastic pipes with length of 800 mm and diameter of 100 mm were connected to the fan outlets to achieve fully developed flow. All the panels were covered with ordinary glasses with a thickness of 5 mm.

.

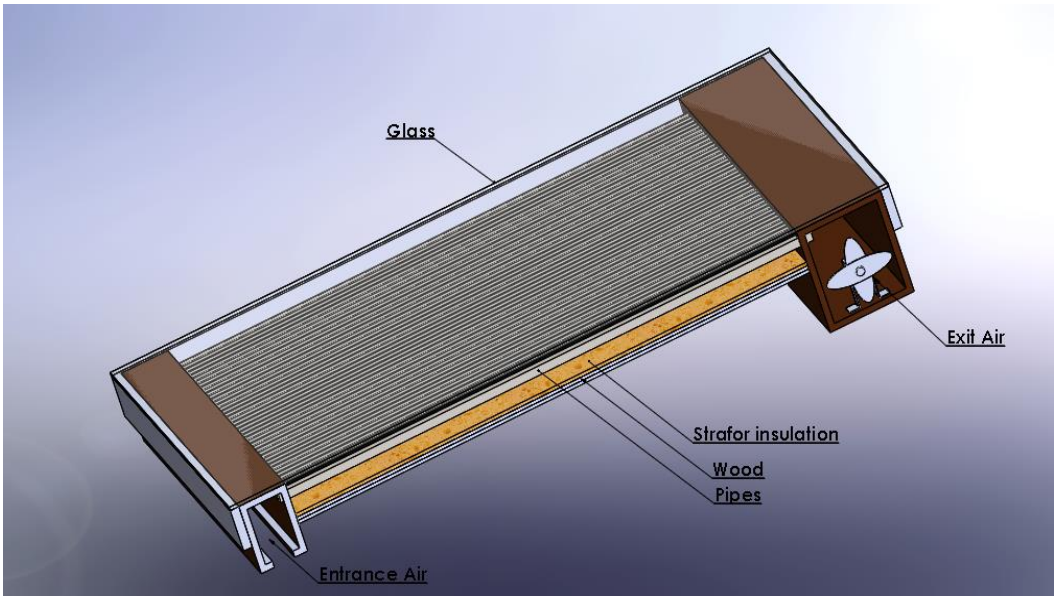

Figure 3.2: Sectional side view of the panels and the parts of the collectors.

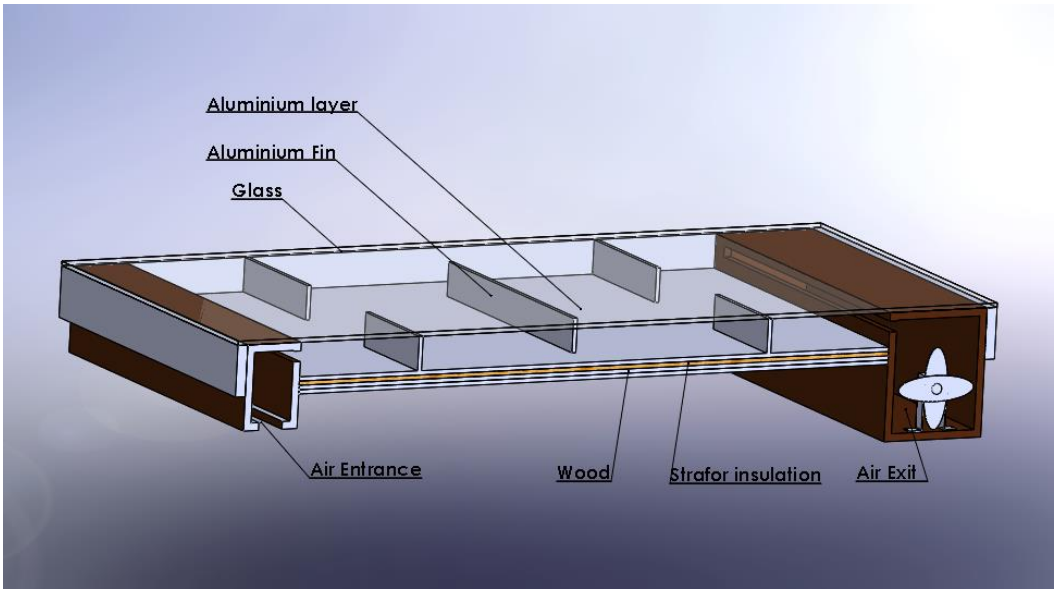

Figure 3.3: Sectional side view of the fins' collector.

3.2 Experimental Equipments Used

3.2.1 Hot Wire Anemometer

This device is used to measure the air velocity. The portable HHF42 wire anemometer was used to measure air velocities (see Fig. 4). The combining aspect of hot wire and standard thermostat delivers fast and accurate measurements even at air velocities with low degrees. The microprocessor circuit assures the maximum possible accuracy and provides special functions and features for this device: ± (5 %+1d), ± 0.8°C [55]. The hot wire anemometer works with the Wheatstone bridge principle [56]. When the flow passes around the calibrated thin wire, cooling effect of the flow changes the resistance of the bridge and this change of the resistance is calculated from the look up table of the system and converted into velocity. The outlet air velocities need to be measured to prevent the effect of the ambient air velocity.

To serve the purpose of the present study, a PVC pipe with a diameter of 100 mm and length of 800 mm as shown in figure [3.4] was attached to the outlet for the air stream to reach the fully developed flow and to prevent the effect of the ambient velocity.

The volumetric flow rate can be calculated by the following equation:

$$Q = A \times V \tag{3.1}$$

Where Q is volumetric flow rate (m^3/s), A is the outlet area (m^2), and V is the outlet velocity (m/s).

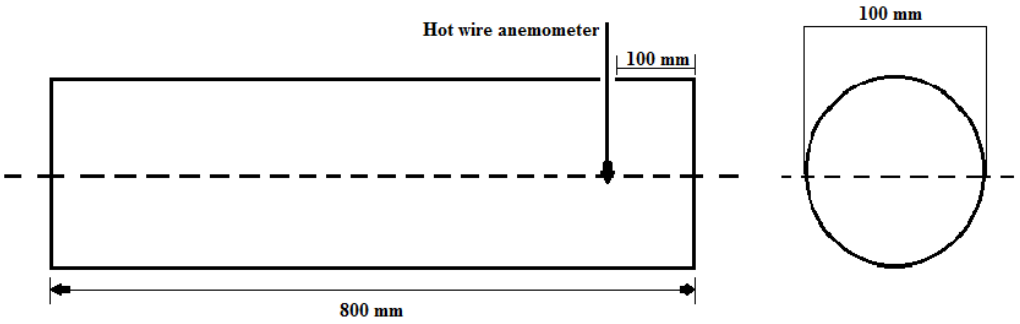

Figure 3.4: The outlet air pipe and hot wire anemometer place.

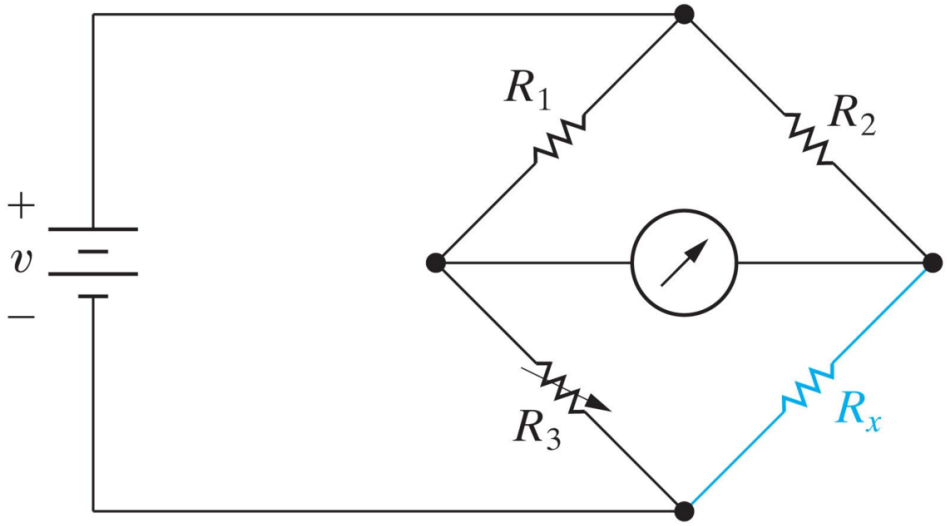

Figure 3.5: Wheatstone bridge circuit diagram [57].

Figure 3.6: Hot Wire Anemometer [58].

3.2.2 Electric Motor Fan

An electric motor centrifugal fan (OBR 200 M-2K) [59], presented in Fig. 3.7 was used in this study to generate high mass flow rate through the collectors. The fan is preferred to be centrifugal to prevent the overheating due to the high temperature of the air coming out from the collectors. Moreover, speed controller was used to control the demand velocities of the air. The motor specifications are presented in Table 3.1

Figure 3.7: Fan with electric motor [60].

Table 1: Specifications of the electric motor fan.

Voltage	**230 V**
Power	**600 W**
Frequency	**50 Hz**
Speed	**2700 Rpm**
Air Flow	**1800 m³/h**
Capacitor	**8 µF/400V**
Insulation Class	**CL F**

3.2.3 Solar Intensity Measurement

A Pyranometer is used to measure the quantity of sun radiation on a designed service. It has a special sensor in order to measure the solar irradiance flux density (W/m^2) from 180 degree field of view. It was connected to HHMIA digital voltmeter which has 0.25 % accuracy and a resolution of ± 0.5 % from 0 to 2800 W/m^2. Factor of conversion is 10.50×10^{-6} V/W m^{-2}. The pyranometer was used to measure the solar irradiance intensity on an inclined surface. The tilt angle of the panel was set as 36^o to get the highest exposure to solar irradiance [61].

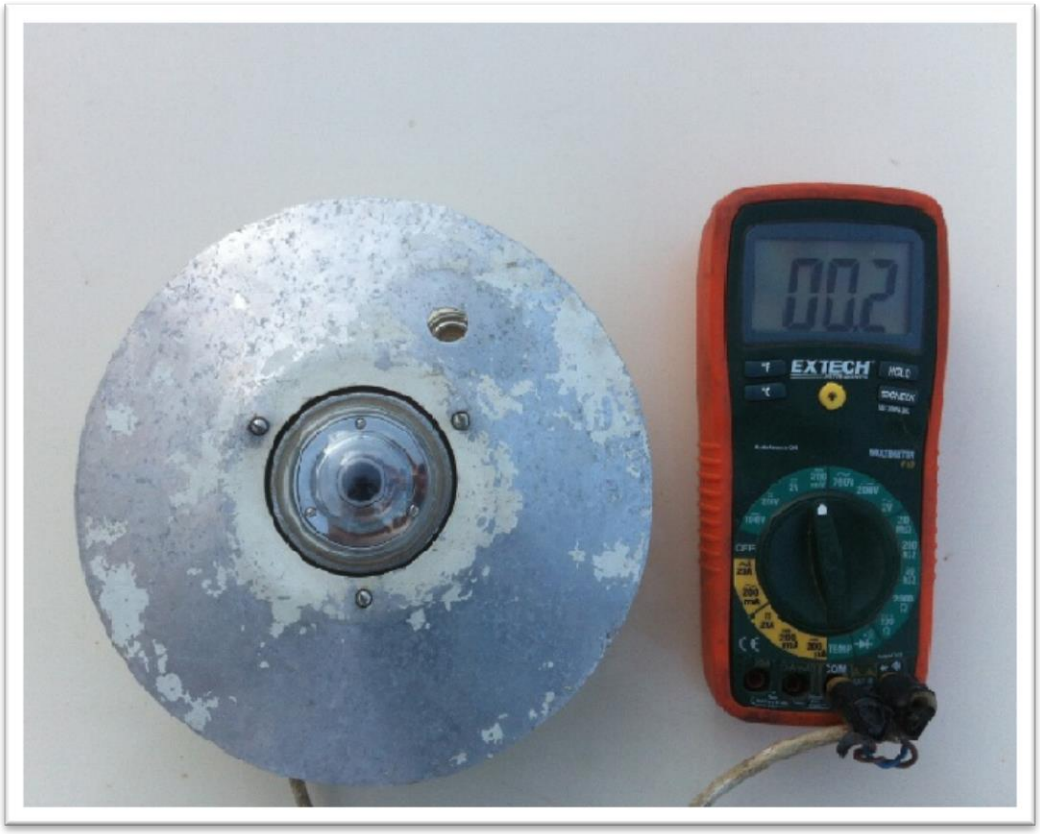

Figure 3.8: View of (Pyranometer).

3.2.4 Thermometer and Temperature Measurements (Xplorer GLX Pasco)

The Xplorer GLX is a tool for data collection, graphing, and analysis. This device is designed for experimentations conducted by science students. The Xplorer GLX supports up to four special sensors simultaneously. Moreover, it has two temperature probes and a voltage probe which are directly connected to the specialized ports. The personal computer devices, such as mouse, keyboard, or printer can be connected to the USB ports of Xplorer of GLX's. The Xplorer GLX contains an integrated speaker for sound generation and another stereo signal output port for amplified speakers as optional headphones. The Xplorer GLX is fully functional and a stand-alone handheld computing device for science. This device works as sensor interface if it is connected to a desktop or laptop computer running Data Studio software [62]. The GLX Xplorer is shown in Fig. 3.9.

Figure 3.9: Xplorer GLX Pasco temperature measurement device [63].

3.2.5 Thermal Analysis and Uncertainty

Throughout the conduct of an experiment a set of data is collected and analyzed based on which the conclusions are made. Uncertainty occurs when the data is not accurate enough or an error is made while measuring the variables and quantities. By using the following equations mass flow rate and thermal efficiency can be calculated;

Mass flow rate ($\dot{m}$) is expressed as:

$$\dot{m} = \rho\, A\, V \tag{3.2}$$

Where, ρ (kg/m$^{3)}$ is the density of air and A (m^2) is the cross sectional area of the pipe at the outlet of the air, V (m/s) is the velocity of the air at the outlet of the device which is measured by using Anemometer.

Uncertainty equation of mass flow rate can be estimated by:

$$\omega_m = \left[\left(\frac{\partial m}{\partial T}\,\omega_T\right)^2 + \left(\frac{\partial m}{\partial P}\,\omega_P\right)^2\right]^{1/2} \tag{3.3}$$

The thermal efficiency (η) of the solar air heater collector panels can be calculated by the following equation expressed as the ratio of the amount of energy gained by the air and the radiation of the sun absorbed by the collector panel:

$$\eta = \frac{\dot{m} C_p\,(T_{out} - T_{in}\ )}{I \mathrm{A_c}} \tag{3.4}$$

As it is presented in the equation, $\dot{m}$ is the mass flow rate, C_p is the specific heat of the fluid, A_c is the collector area, T_{in} is air temperature of the fluid at the entrance; T_{out} is air temperature of the fluid at the exit.

The uncertainty for efficiency ($\omega\eta$) is a function of $\dot{m}$, ΔT and I, assuming that A_c, and C_p are constants.

$$\omega_\eta = \left[\left(\frac{\partial \eta}{\partial \boldsymbol{m}}\omega_m\right)^2 + \left(\frac{\partial \eta}{\partial \boldsymbol{\Delta T}}\omega_{\Delta T}\right)^2 + \left(\frac{\partial \eta}{\partial \boldsymbol{I}}\omega_I\right)^2\right]^{1/2} \quad (3.5)$$

Chapter 4

RESULTS AND DISCUSSION

The three collectors were experimentally investigated under the climatic conditions of Famagusta during the summer season between 12.07.2013 and 30.07.2013. The weather was clear and the wind velocities were negligible during the test period. The three SAHs were placed at the same place so the conditions were same for all the collectors. The city of Famagusta is located in Turkish Republic of North Cyprus at the longitudes of 35.125^{o} N and 33.95^{o} E. The thermal performance of the three collectors has been inspected and compared with previous studies to find the most effective device deployed in the study.

4.1 Solar Intensity

Solar intensity is the amount of solar power (energy from the sun per unit of time) per unit area reaching a location of interest. The unit of the intensity is W/m^2. The figure below shows the daily average of the solar intensity during the experiment's period. The results show that the maximum intensity of the daily solar irradiance obtained is 871.43 W/m^2 at 13:00 hrs. The average of solar intensity during the study period is presented in Fig 4.1.

4.2 Effect of the mass flow rate and the Different Absorber Plates inside the Collectors

Experiments were carried out for different types of absorber media and different mass flow rates. The solar air heater collectors were investigated experimentally. The temperature differences between the inlet and exit of the SAHs for different mass flow rates are presented in Figs. 4.2 - 4.12. It is evident that as the mass flow rates increase, the temperature difference decreases.

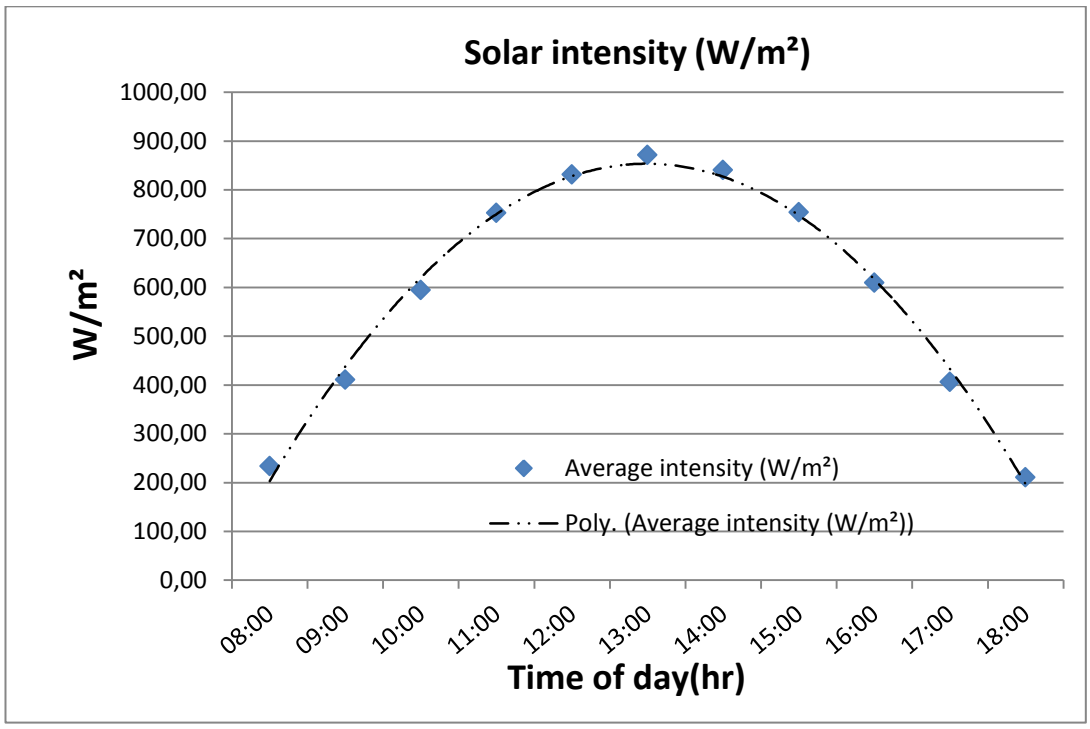

Figure 4.1: Average of solar intensity during the study (12-30/07/2013).

It should be noted that the inlet and exit temperatures of the collectors were measured three times for each mass flow rate and then an average temperature data was obtained. For the collector with fins, the maximum temperature difference during the study period was 26.8 °C at 0.02 kg/s mass flow rate as shown in Fig. 4.2. For the collector with (20mm x 20mm) aluminum tubes, the maximum temperature difference obtained was 29.4 °C, as illustrated in Fig. 4.3. The maximum temperature difference measured for the collector with (25mm x 25mm) square aluminum tubes was 29.5 °C as shown in Fig. 4.4. All maximum temperature differences were observed at the middle of the day at 13:00 (hrs). The results showed that the temperature difference increases depending on the solar radiation striking the collectors, if the mass flow rate is equal for all the collectors being investigated.

In a previous study which investigated the efficiency of a single pass solar air heater functioning under the prevailing weather conditions of Famagusta during the summer season, showed a maximum temperature difference of 27 °C at 0.012 kg/s at 13:00 (hr) and the maximum thermal efficiency obtained as 45.93% at the highest mass flow rate 0.038 kg/s. The highest daily solar radiation obtained was 1050 W/m2 at 13:00 (hr) as shown in figure.4.2. [64].

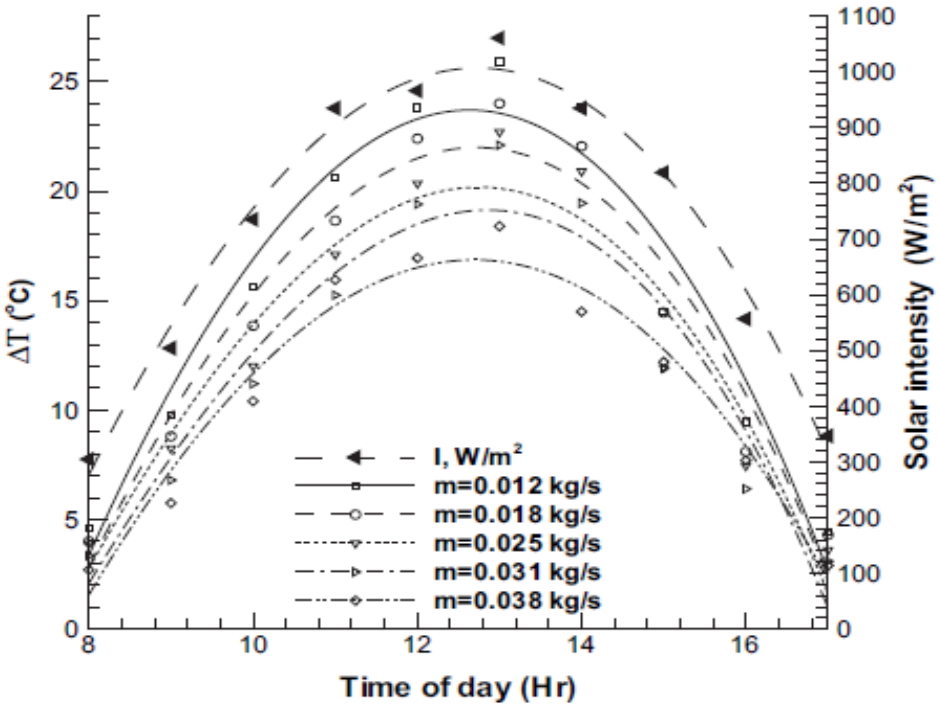

Figure 4.2: Outlet and inlet air temperature difference versus time of the day for different mass flow rates and hourly measured solar radiation - single pass collector [65]

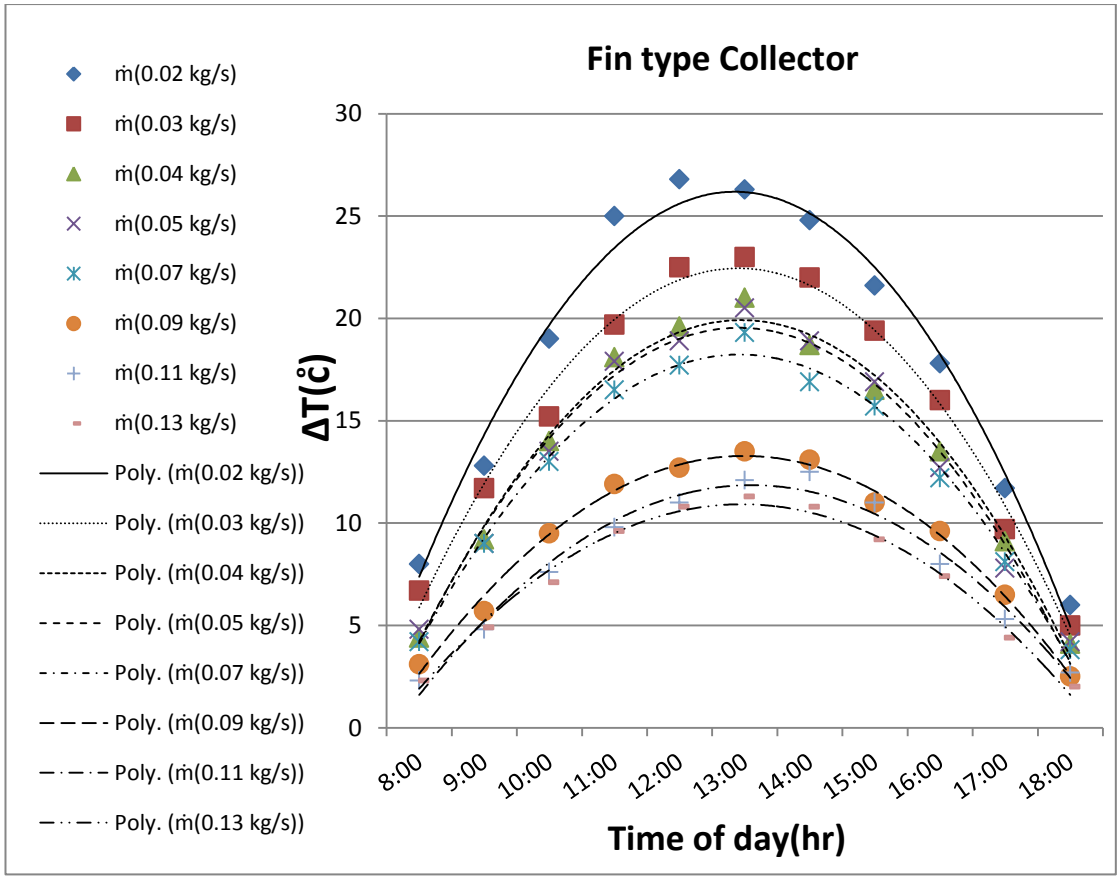

Figure 4.3: The temperature difference between the outlet and inlet air against time for different mass flow rates during the period of the study (12-30/07/2013).

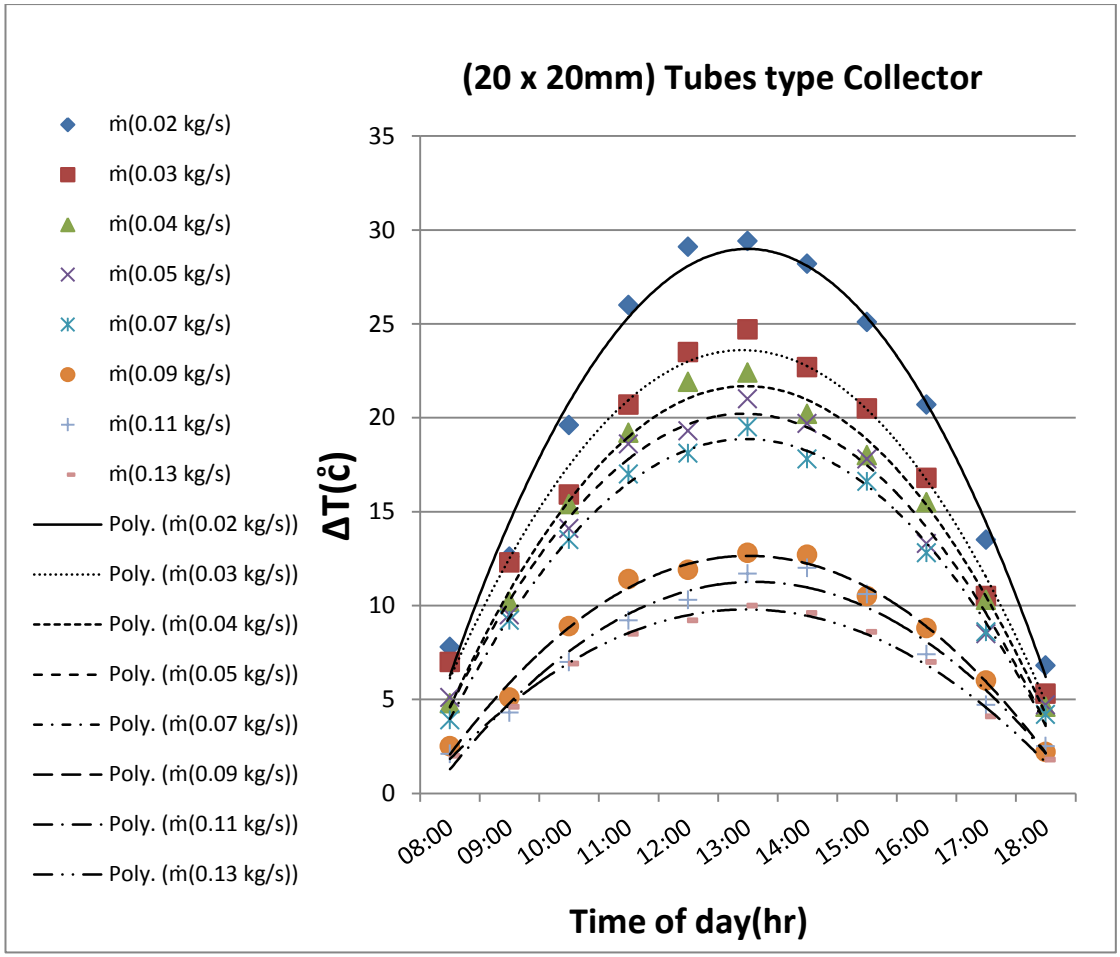

Figure 4.4: The temperature difference between the outlet and inlet air against time for different mass flow rates during the period of the study (12-30/07/2013).

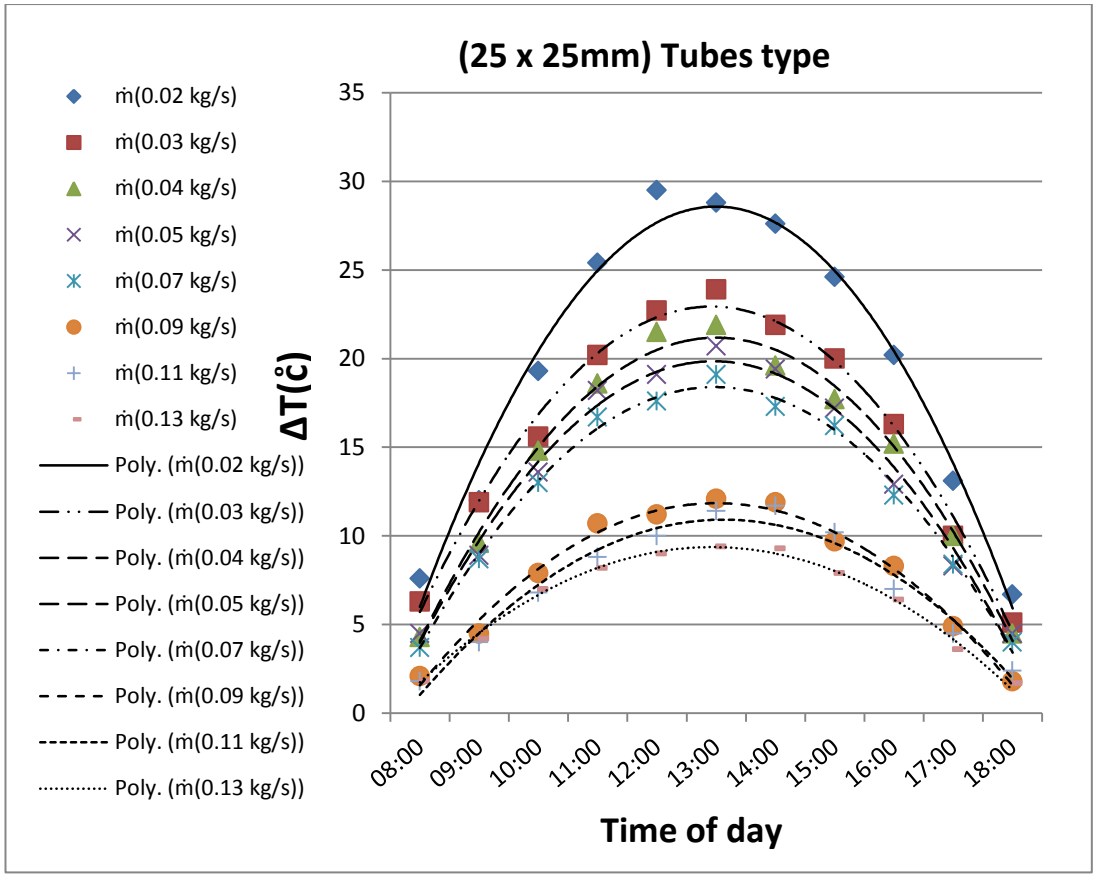

Figure 4.5: The temperature difference between the outlet and inlet air against time for different mass flow rates during the period of the study (12-30/07/2013).

4.3 The temperature difference of the collectors at the same mass flow rates

In this section temperature readings of all type of collectors are plotted for daily reading intervals. The readings are taken for each mass flow rate separately.

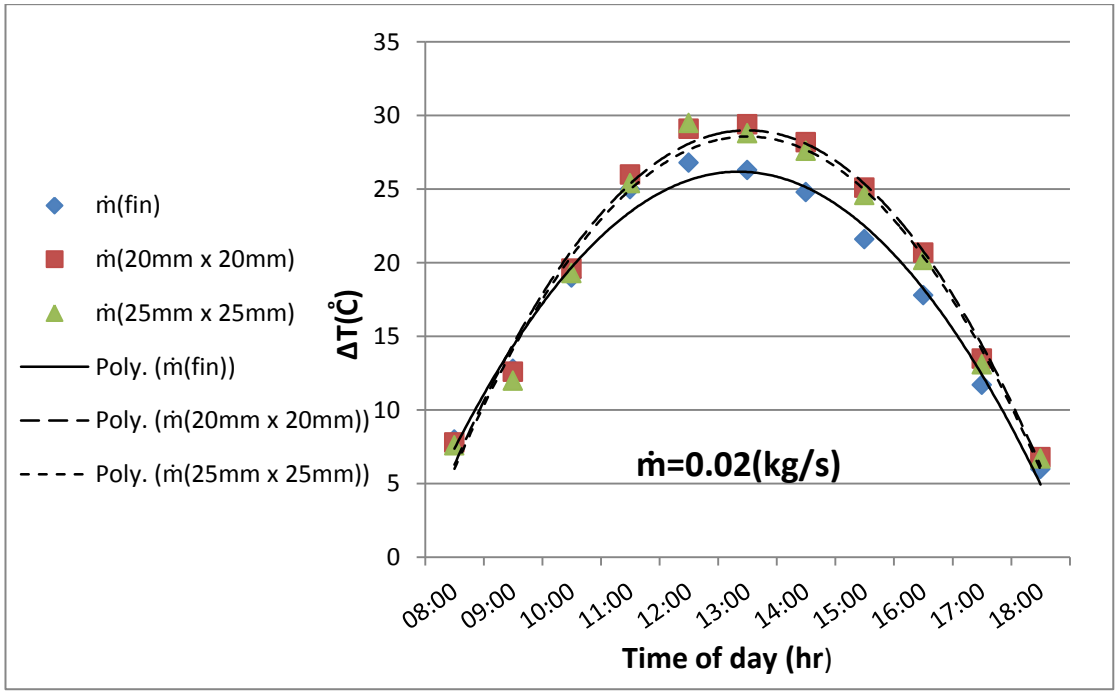

Figure 4.6: The temperature difference between the outlet and inlet air at 0.02 kg/s against time in a day (12/7/2013).

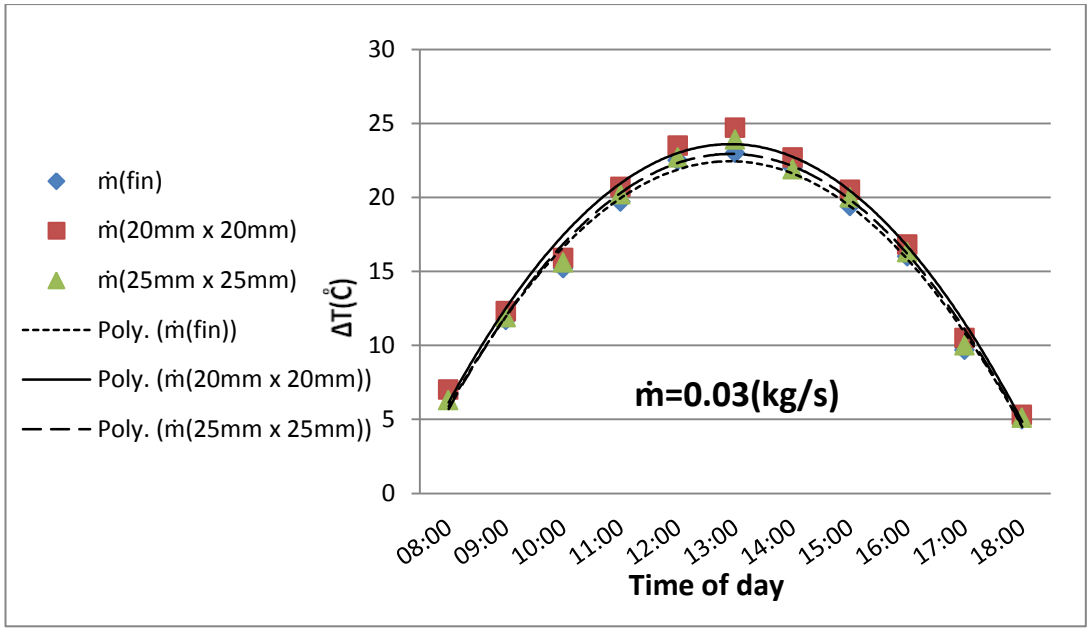

Figure 4.7: The temperature difference between the outlet and inlet air at 0.03 kg/s against time in a day (13/7/2013).

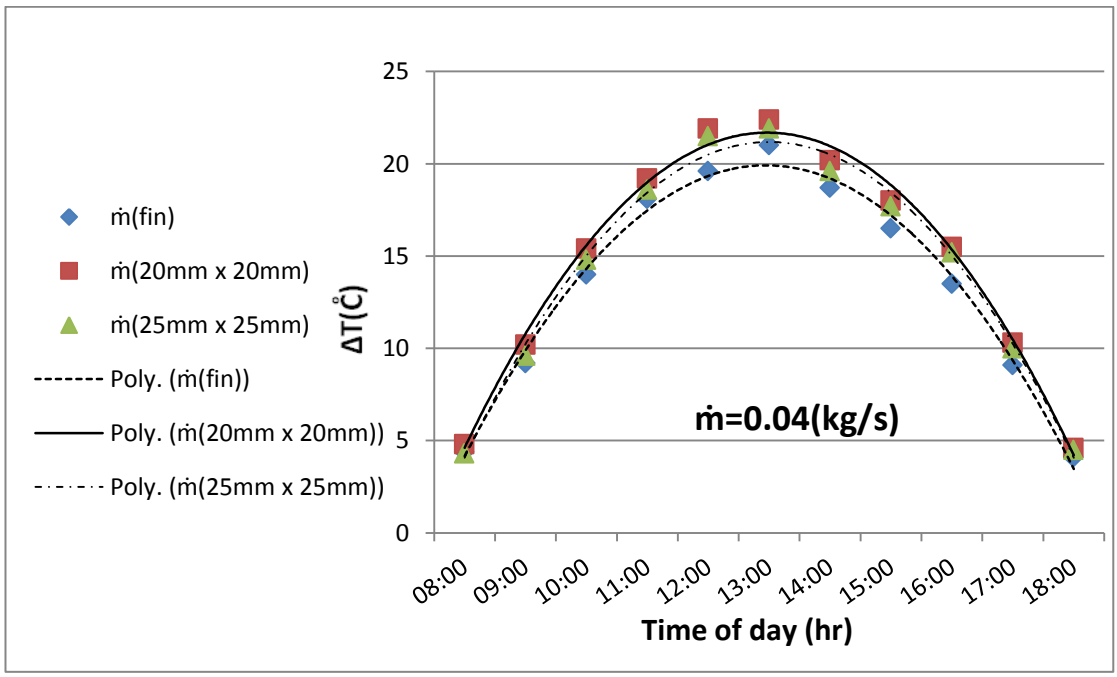

Figure 4.8: The temperature difference between the outlet and inlet air at 0.04 kg/s against time in a day (14/7/2013).

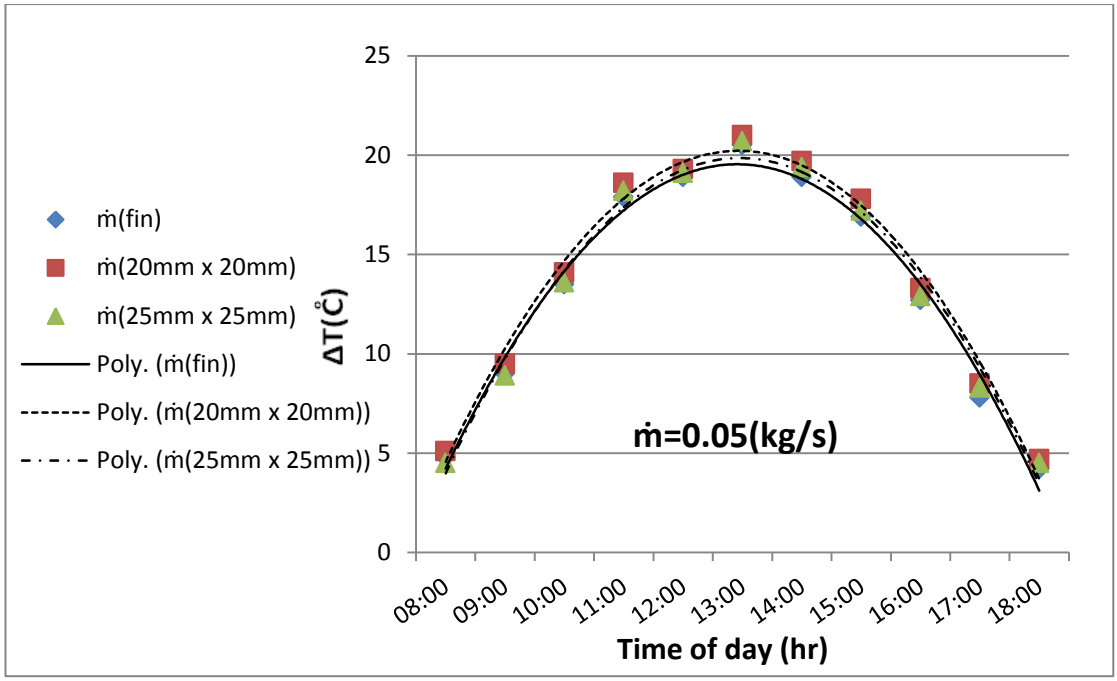

Figure 4.9: The temperature difference between the outlet and inlet air at 0.05 kg/s against time in a day (15/7/2013).

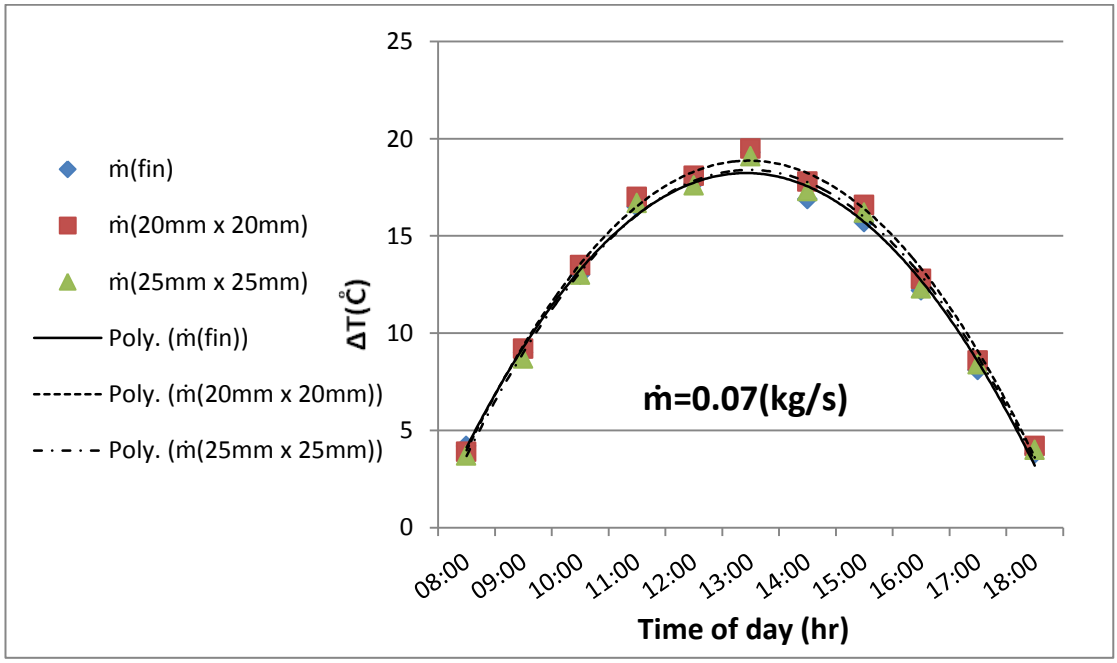

Figure 4.10: The temperature difference between the outlet and inlet air at 0.07 kg/s against time in a day (23/7/2013).

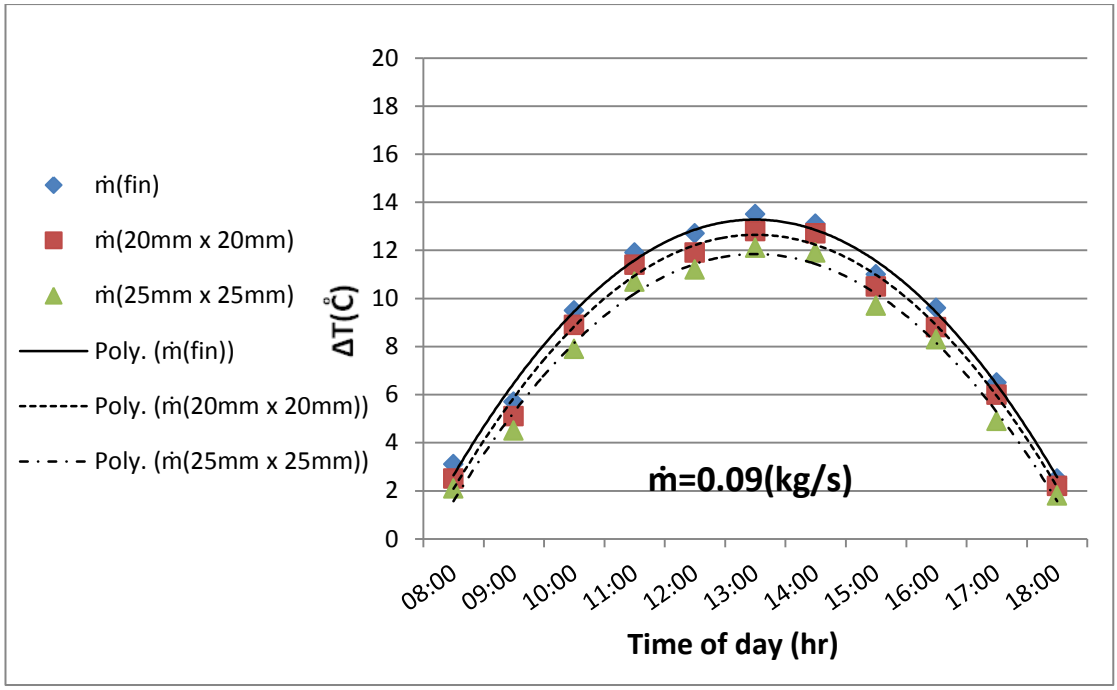

Figure 4.11: The temperature difference between the outlet and inlet air at 0.09 kg/s against time in a day (25/7/2013).

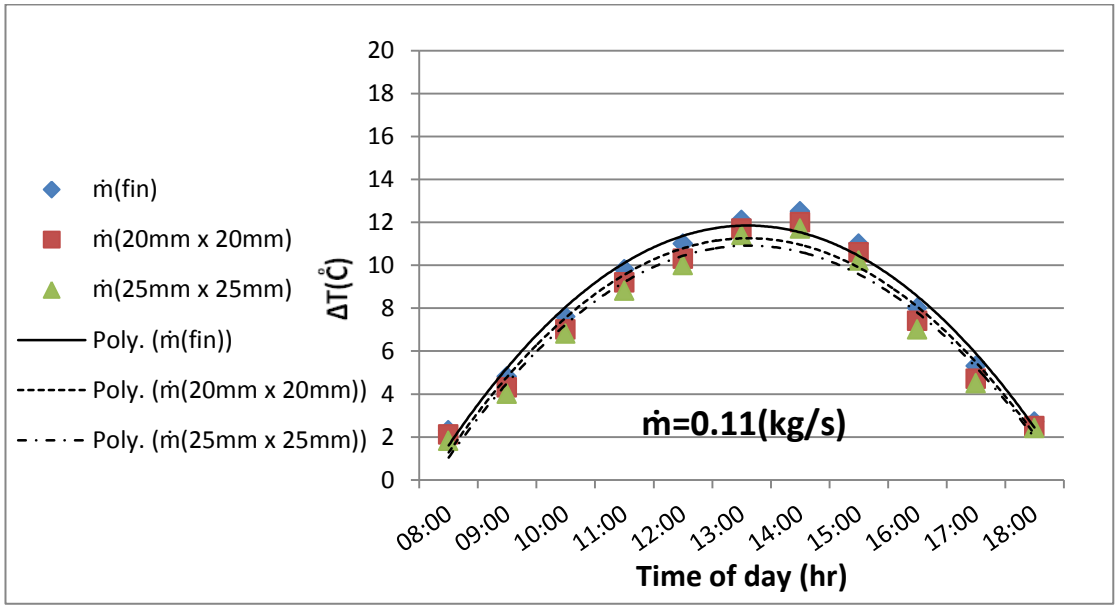

Figure 4.12: The temperature difference between the outlet and inlet air at 0.11 kg/s against time in a day (27/7/2013).

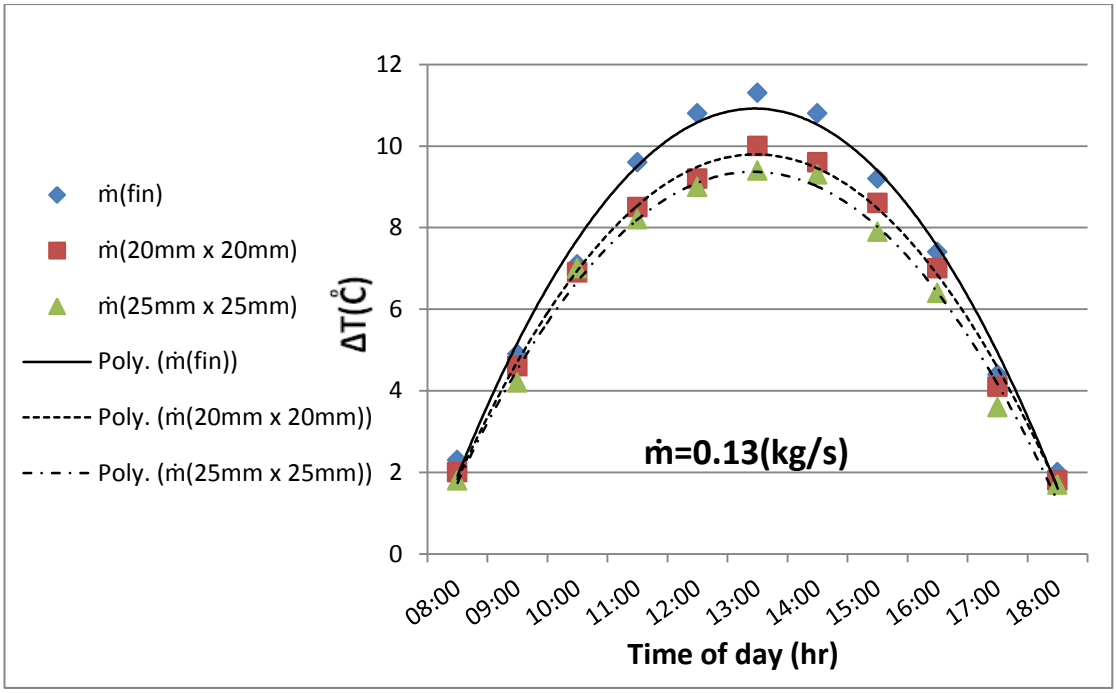

Figure 4.13: The temperature difference between the outlet and inlet air at 0.13 kg/s against time in a day (29/7/2013).

4.4 Normalization of the Temperature data

The aspect of data normalization has been used to compare the results between present study and literature.

The calculations for temperature data normalization have been done for three different mass flow rates. The temperature data normalization calculations for the present study collectors have showed that there is no big difference between the three SAHs collectors.

Data Normalization can be calculated by using this equation [66]:

$$X_{i,\,0:1} = (X_i - X_{Min}) / (X_{Max} - X_{Min}) \qquad (4.1)$$

Where:

X_i = Each data point i.

X_{Min} = The minimum among all the data points.

X_{Max} = The maximum among all the data points.

$X_{i,\,0\ to\ 1}$ = The data point i normalized between 0 and 1.

For the fin's collector at (0.02 kg/s) the normalization obtained as $X_{\mathbf{i,\,0:1}} = 0.58$ and for (20 x 20 mm and 25 x 25 mm) tubes type collectors the normalization have calculated as $X_{\mathbf{i,\,0:1}} = 0.58$ and $X_{\mathbf{i,\,0:1}} = 0.56$ respectively, also for the wire mesh collector it calculated as $X_{\mathbf{i,\,0:1}} = 0.48$ as shown in figure (4.13).

At (0.03 kg/s) For the fin's collector the normalization obtained as $X_{i,\ 0:1}$= 0.59 and for (20 x 20 mm and 25 x 25 mm) tubes type collectors the normalization have obtained as $X_{i,\ 0:1}$ = 0.7 in addition for the wire mesh collector it reached $X_{i,\ 0:1}$ = 0.45 as shown in figure (4.14).

For the fin's collector at (0.04 kg/s) the normalization obtained as $X_{i,\ 0:1}$ = 0.55 and for (20 x 20 mm and 25 x 25 mm) tubes type collectors the normalization have calculated as $X_{i,\ 0:1}$ = 0.58 and $X_{i,\ 0:1}$ = 0.57 respectively, moreover for the wire mesh collector it is obtained as $X_{i,\ 0:1}$ = 0.47 as shown in figure (4.15).

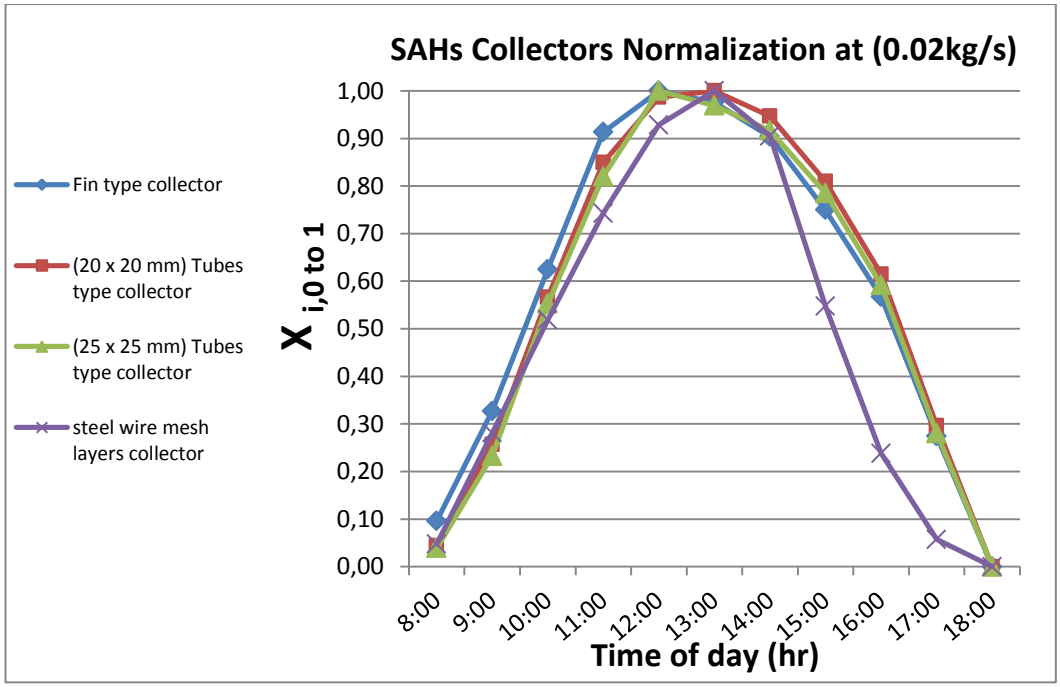

Figure 4.14: The temperature data normalization for the SAHs collectors at 0.02 kg/s.

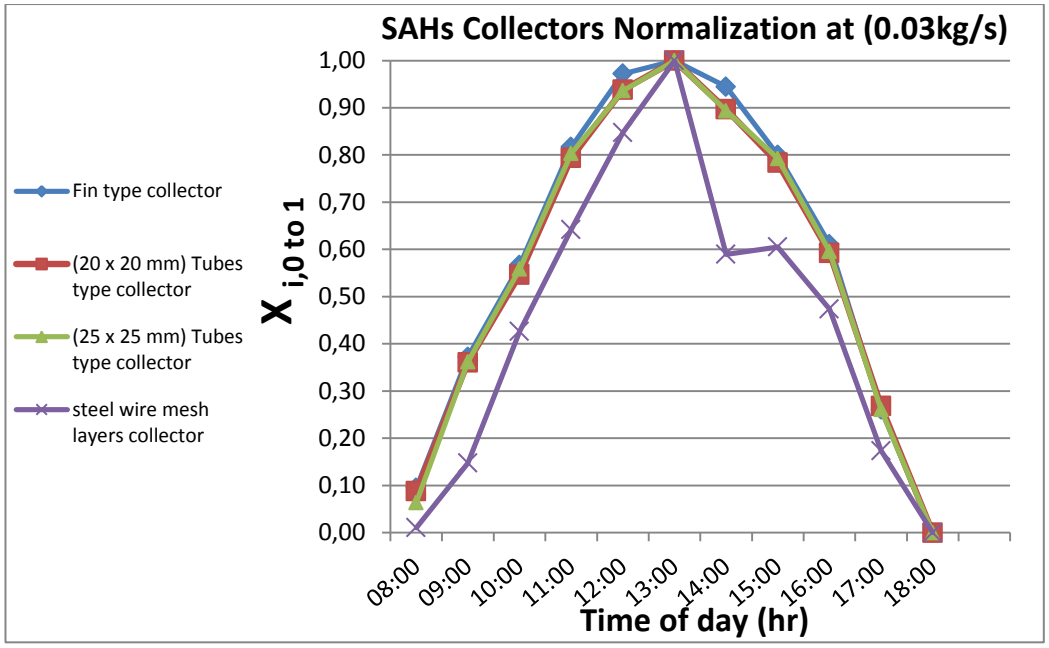

Figure 4.15: The temperature data normalization for the SAHs collectors at 0.03 kg/s.

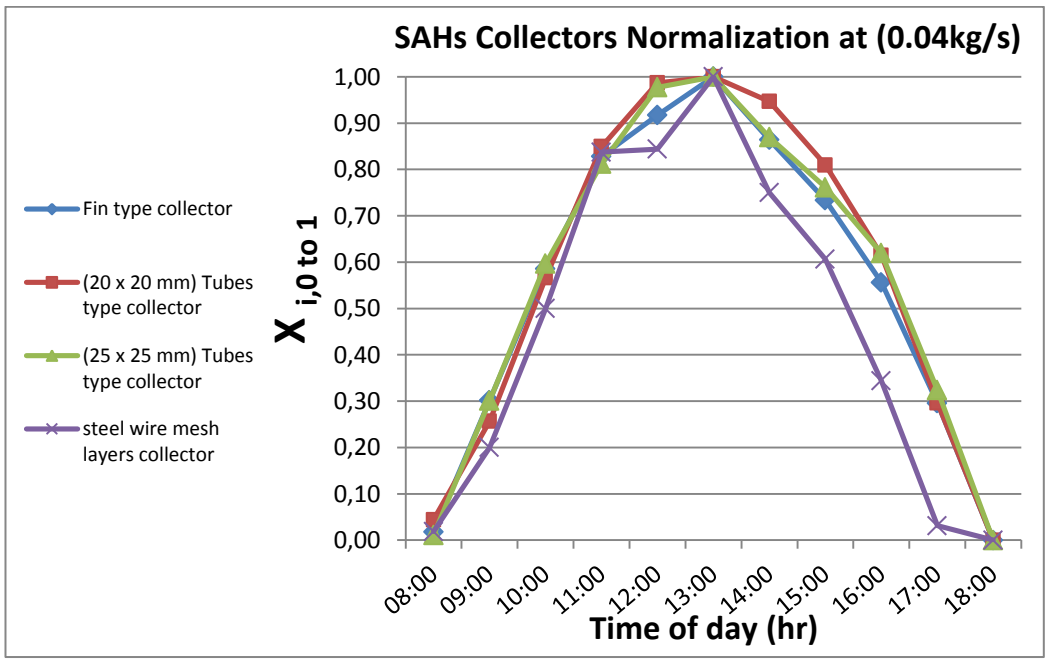

Figure 4.16: The temperature data normalization for the SAHs collectors at 0.04 kg/s.

4.5 The Thermal Efficiency of the Collectors

The results of efficiency against time at different mass flow rates for three different types of SAHs are showed in Figs. (4.13- 4.15) below. The results indicate that the growth of thermal efficiencies of the collectors is synchronized with the increase in mass flow rate of the air. For the collector with fins the results showed that the maximum efficiency obtained is 93% at 0.13kg/s mass flow rate at 13:00 hrs. The maximum efficiencies for the (20 x 20mm) and (25 x 25mm) square aluminium tubes were calculated as 86% and 84%, respectively for the mass flow rate of 0.07 kg/s.

For fin's collector at 0.04 kg/s the maximum efficiency reached 54.15% and for (20 x20 mm and 25 x 25 mm) at same mass flow rate the highest efficiency obtained as 58.36% and 56.19% respectively.

In a previous study which investigated the efficiency of a single pass solar air heater collector under Famagusta weather conditions during the summer month 15.06.2009 - 15.07.2009, showed a maximum thermal efficiency as 45.93 % at 0.038 kg/s mass flow rate [67].

By comparing the efficiency results for the present study and the old study at 0.04 kg/s, the researcher found that the new SAHs collectors have showed better thermal performance than the old one.

For the fin type collector the maximum efficiency was calculated at the maximum mass flow rate, because all the energy is transferred to the fluid directly by radiation and convection. Where for the tube type collectors the maximum efficiency was obtained at 0.07 kg/s because here energy is transferred to the tubes by radiation and from tube to the fluid by convection. This is the reason in reduction of efficiency.

4.5.1 Thermal Efficiency Performance of the Collectors

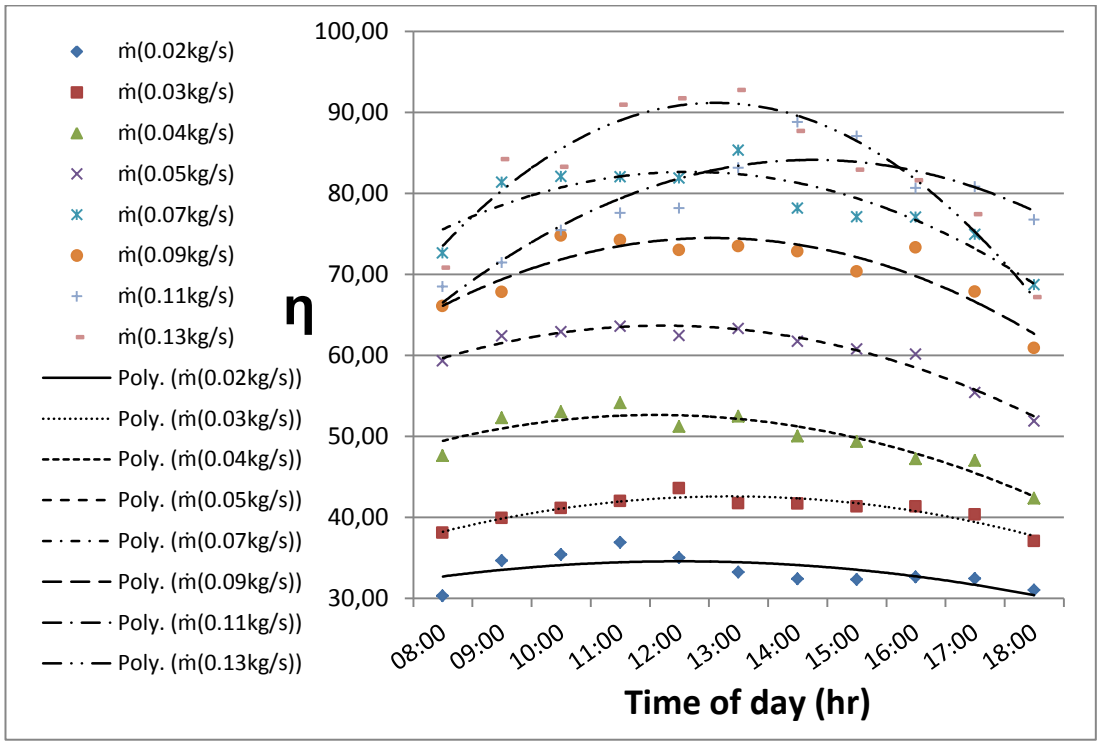

Figure 4.17: Efficiency performance at various times and different mass flow rates for the collector with fins.

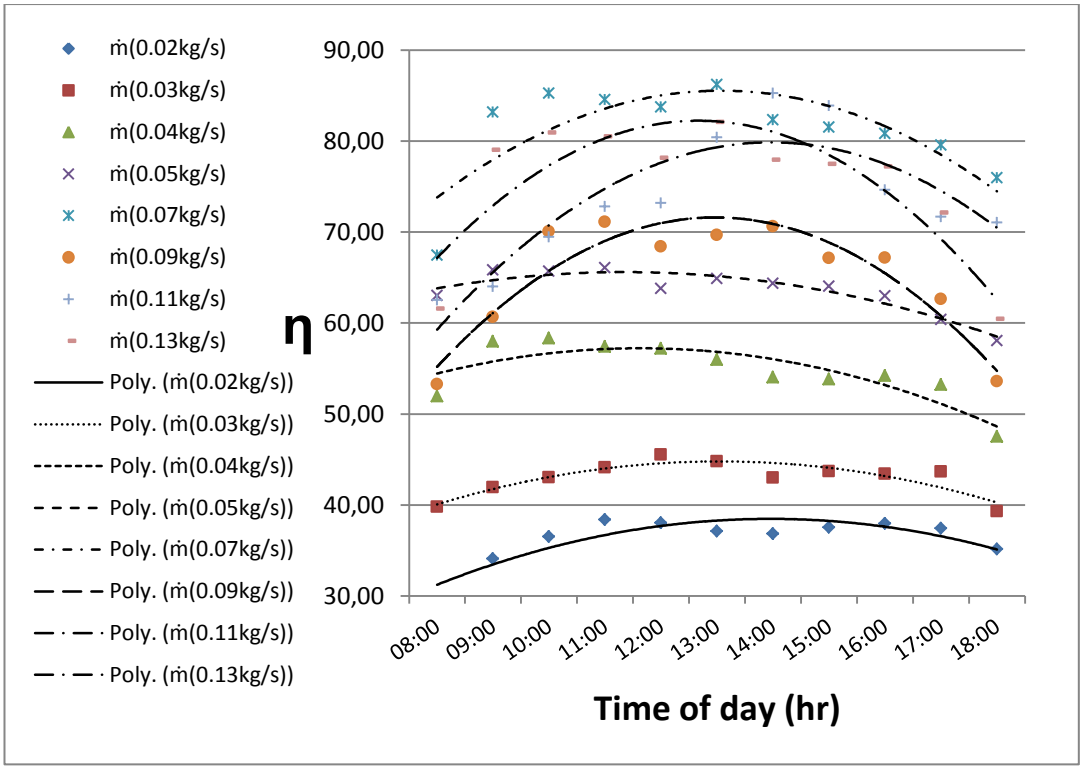

Figure 4.18: Efficiency performance at various times and different mass flow rates for the collector with (20 x 20mm) aluminium tubes.

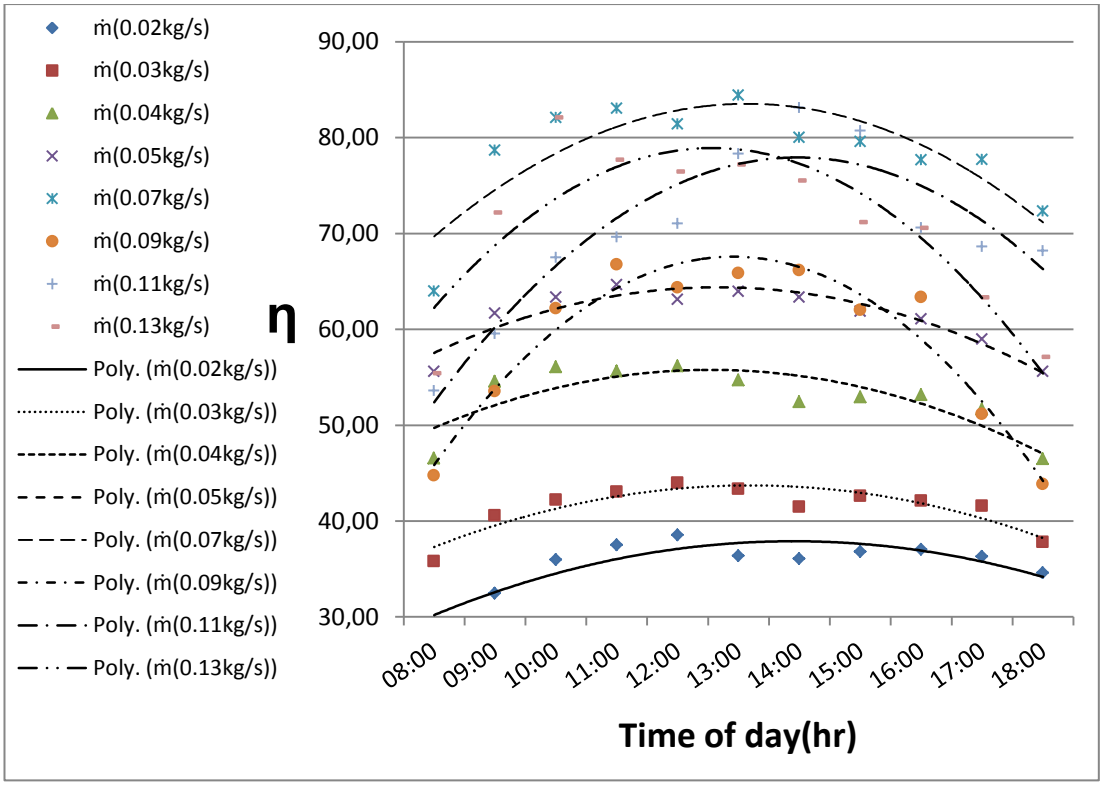

Figure 4.19: Efficiency performance at various times and different mass flow rates for the collector with (25 x 25mm) aluminium tubes.

The thermal efficiencies of the collectors with the same mass flow rates are presented in Figs. (4.16 - 4.23). The thermal efficiencies of the tube collectors were higher compared with finned flat plate collector when the mass flow rates were 0.07 kg/s or less. As the mass flow rate increased above 0.07 kg/s, the finned flat plate solar collector performed better compared with tube type collectors. It is worth to note that the 20 x 20 mm tube collector performed better than 25 x 25 mm tube collector. This is because of in narrow area particles are accelerated and carrying more energy than those which are slower.

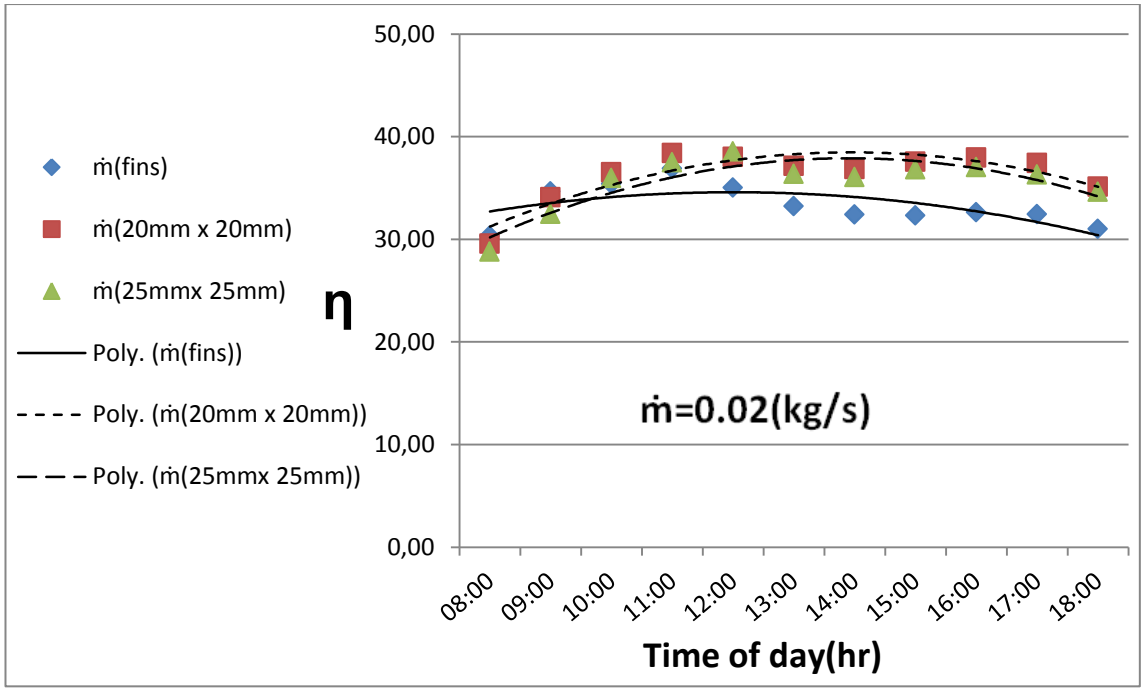

Figure 4.20: Efficiency of the collectors at 0.02(kg/s).

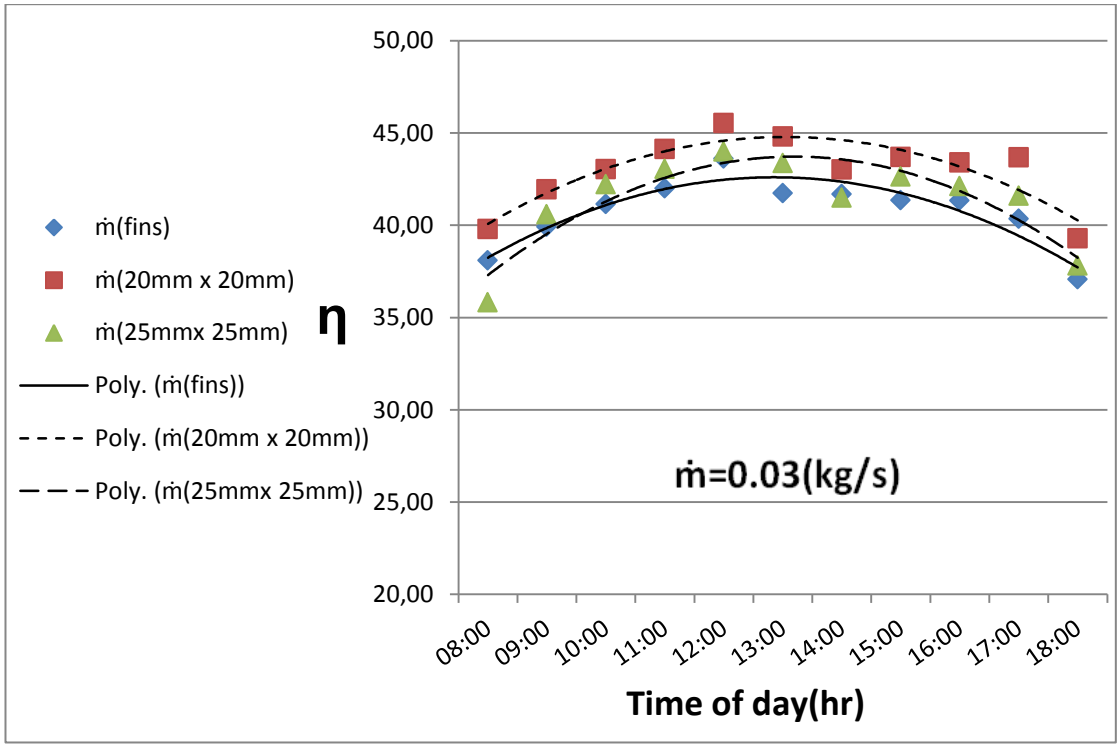

Figure 4.21: Efficiency of the collectors at 0.03(kg/s).

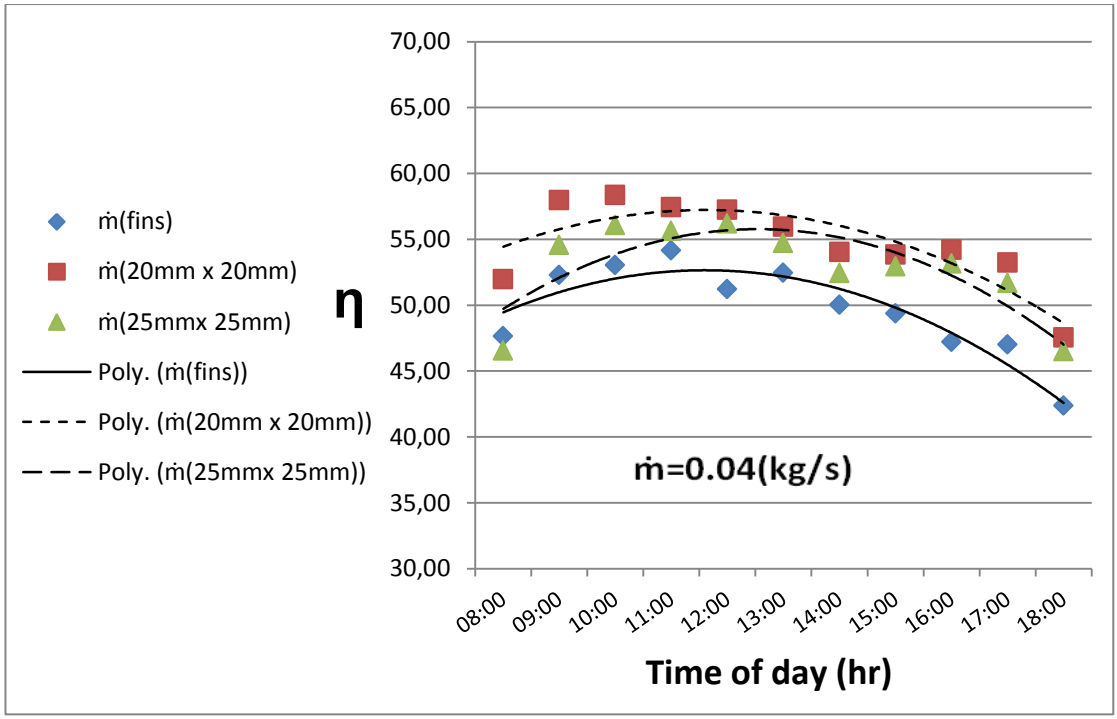

Figure 4.22: Efficiency of the collectors at 0.04(kg/s).

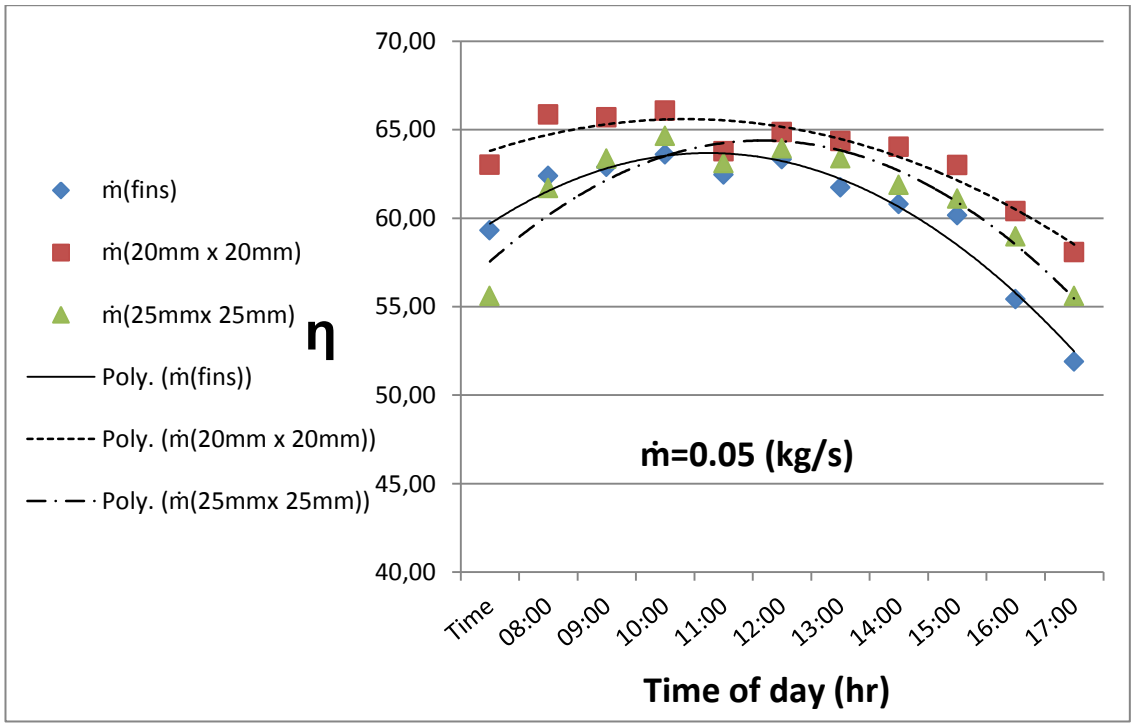

Figure 4.23: Efficiency of the collectors at 0.05(kg/s).

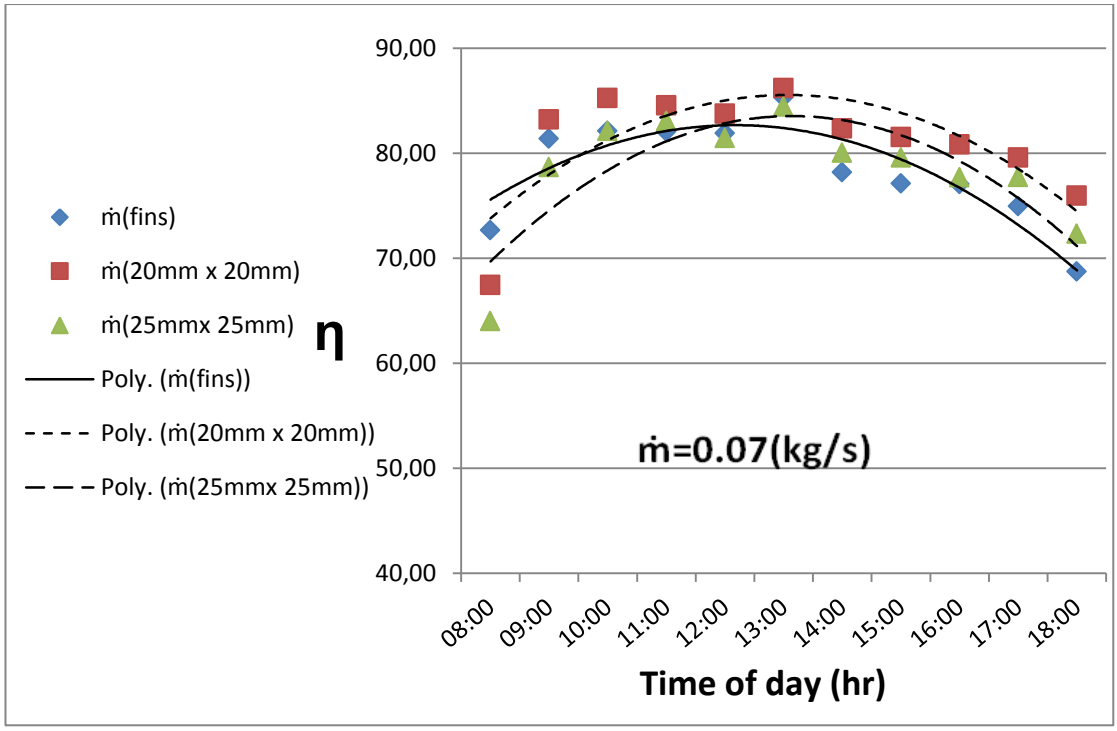

Figure 4.24: Efficiency of the collectors at 0.07(kg/s).

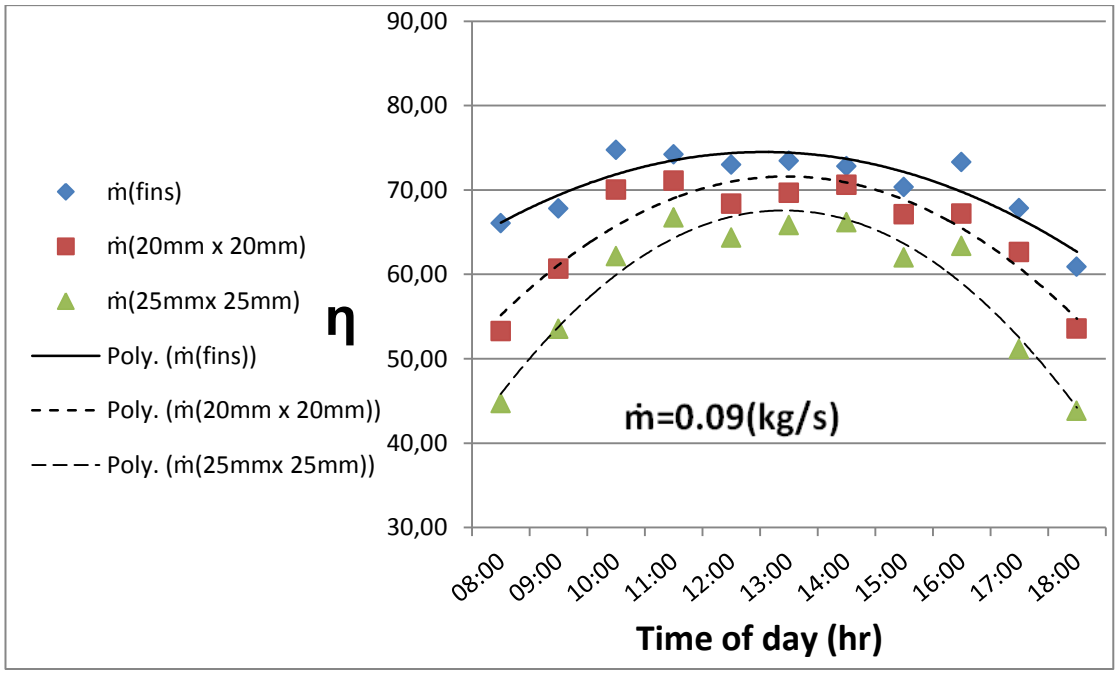

Figure 4.25: Efficiency of the collectors at 0.09(kg/s).

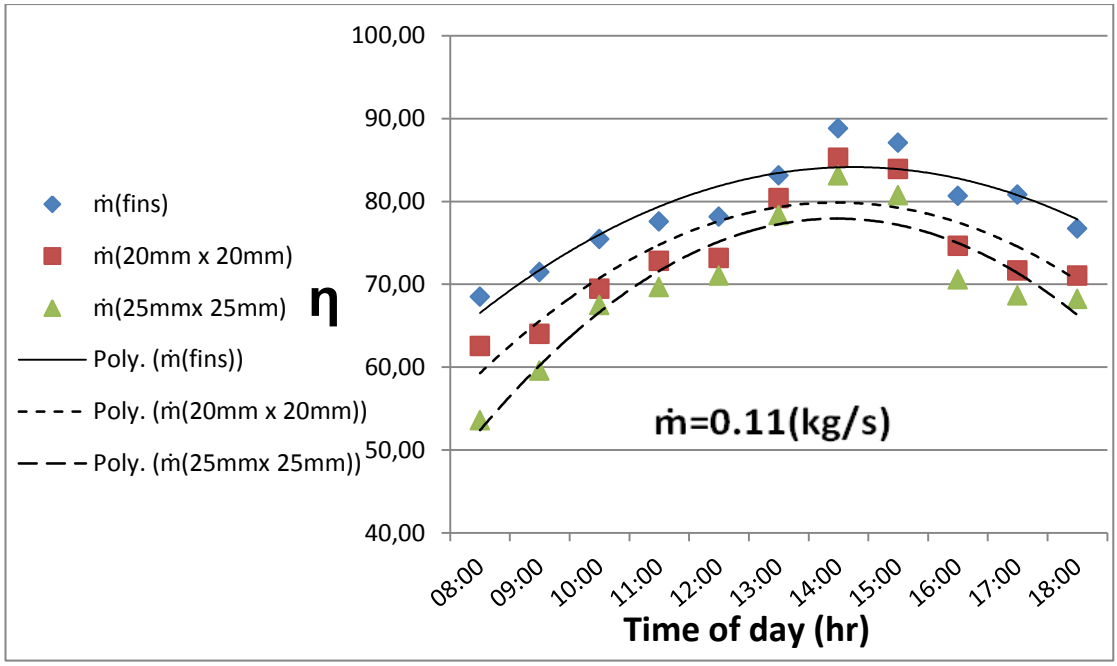

Figure 4.26: Efficiency of the collectors at 0.11(kg/s).

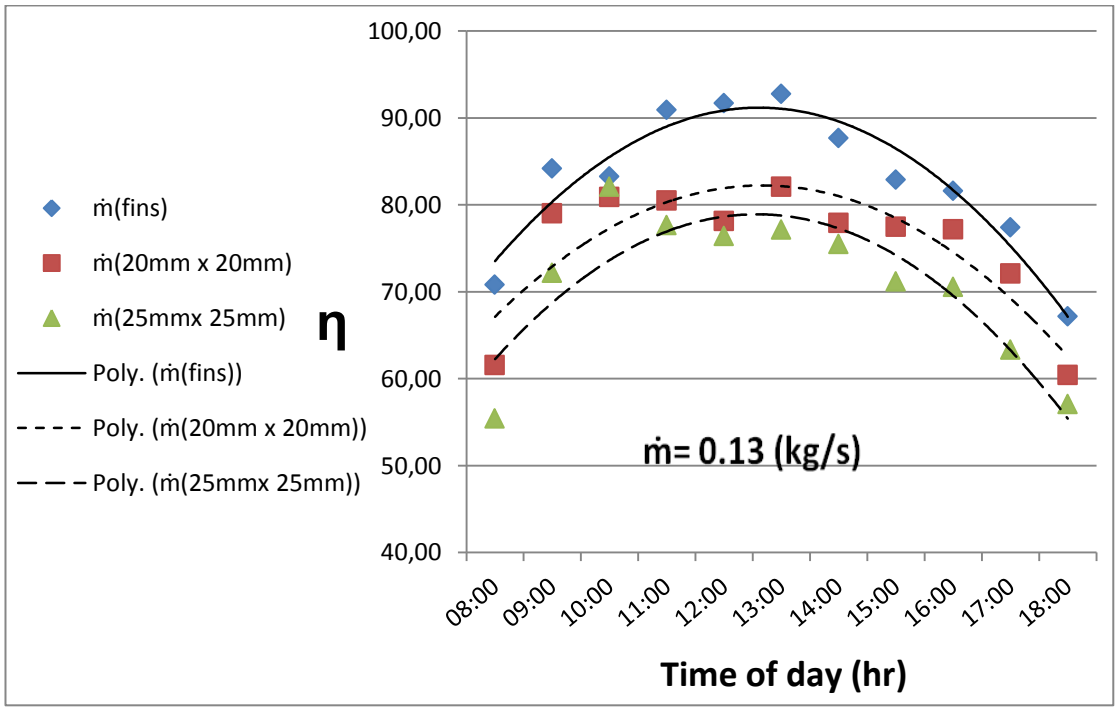

Figure 4.27: Efficiency of the collectors at 0.13(kg/s).

Chapter 5

CONCLUSION AND RECOMMENDATIONS

The main aim of the present study was to investigate the thermal performance of three SAHs built at the EMU mechanical workshop. The experiments were carried out in the setting of Mechanical Engineering Department at Eastern Mediterranean University in the city of Famagusta in July, 2013.

Based on the obtained results, it can be claimed that the performance of the SAHs was significant. The finned type collector achieved the maximum temperature difference as $\Delta T = 26.8\ C^o$ at 0.02 kg/s, and the maximum thermal efficiency was calculated as 93% at 0.13 kg/s. The maximum temperature difference for (20mm x 20mm) collector was measured as $\Delta T = 29.4\ C^o$ at 0.02 kg/s and the highest thermal efficiency was estimated as 86.21% at 0.07kg/s. For the (25mm x 25mm) collector the maximum difference of temperature was revealed as $\Delta T = 29.5\ C^o$ at 0.02 kg/s and, the thermal efficiency was measured as 84.44% at 0.07 kg/s. In addition, according to the results it was found that compared with the single pass SAHs which were constructed and implemented previously in Famagusta, the SAHs investigated in the present study functioned better in terms of performance. However, when the three SAHs normalised data`s were compared with each other, it was revealed that the smaller sized tube type collector performed better than the other tube type collector. Overall, the finned flat plate collector had a more desirable performance at higher mass flow rates compared to the tube collectors.

5.1 Suggestions for Future Work Studies

To increase the effectiveness of the SAHs, two pass solar heaters can be employed. Thus, two pass SAHs which are consist of a transparent covers located between the top glazing and the collector can be constructed and investigated in future studies.

REFERENCES

[1] "Survey of Active Solar Thermal Collectors, Industry and Markets in Canada",*NaturalResourcesCanada*,http://canmetenergy.nrcan.gc.ca/renewables/solar-thermal/publications/3005, (Accessed on May 12, 2013).

[2] Wazed, M. A., Nukman, Y., & Islam, M. T., "Design and fabrication of a cost effective solar air heater for Bangladesh," *Applied Energy*, *87*(10), 3030-3036, (2010).

[3] "Solar Air Heating," *World Industries Association (SAT-IWIA*), http://www. Sahwia.org, (Accessed on April 15, 2013).

[4] De Saussure, H., "2500 Years of Solar Architecture and Technology," (http://vvww.solarcooking.org/saussure.htm), (Accessed on April 15, 2013).

[5] Mohamad, A. A., "High efficiency solar air heater." *Solar Energy*, *60*(2), 71-76, (1997).

[6] Garg, H. P., Jha, R., Choudhury, C., & Datta, G., "Theoretical analysis on a new finned type solar air heater," *Energy*, *16*(10), 1231-1238, (1991).

[7] Choudhury, C., Andersen, S. L., & Rekstad, J., "A solar air heater for low temperature applications," *Solar Energy*, *40*(4), 335-343, (1988).

[8] Swartman, R. K., & Ogunlade, O., "An investigation on packed-bed collectors," *Solar energy*, *10*(3), 106-110, (1996).

[9] Sharma, S. P., Saini, J. S., & Varma, H. K., "Thermal performance of packed-bed solar air heaters," *Solar energy*, *47*(2), 59-67, (1991).

[10] Kabeel, A. E., & Mečárik, K., "Shape optimization for absorber plates of solar air collectors." *Renewable energy*, *13*(1), 121-131, (1998).

[11] San Martin, R. L., & Fjeld, G. J., "Experimental performance of three solar collectors," *Solar Energy*, *17*(6), 345-349, (1975).

[12] Prasad, S. B., Saini, J. S., & Singh, K. M., "Investigation of heat transfer and friction characteristics of packed bed solar air heater using wire mesh as packing material," *Solar Energy*, *83*(5), 773-783, (2009).

[13] Sopian, K., Daud, W. R. W., Othman, M. Y., & Yatim, B., "Thermal performance of the double-pass solar collector with and without porous media," *Renewable Energy*, *18*(4), 557-564, (1991).

[14] Naphon, P., "Effect of porous media on the performance of the double-pass flat plate solar air heater," *International communications in heat and mass transfer*, *32*(1), 140-150, (2005).

[15] Ho, C. D., Yeh, H. M., & Wang, R. C. (2005), "Heat-transfer enhancement in double-pass flat-plate solar air heaters with recycle," *Energy, 30*(15), 2796-2817, (2005).

[16] Lertsatitthanakorn, C., Khasee, N., Atthajariyakul, S., Soponronnarit, S., Therdyothin, A., & Suzuki, R. O., "Performance analysis of a double-pass thermoelectric solar air collector," *Solar Energy Materials and Solar Cells*, *92*(9), 1105-1109, (2008).

[17] Esen, H., "Experimental energy and exergy analysis of a double-flow solar air heater having different obstacles on absorber plates," *Building and Environment, 43*(6), 1046-1054, (2005).

[18] Ozgen, F., Esen, M., & Esen, H., "Experimental investigation of thermal performance of a double-flow solar air heater having aluminium cans," *Renewable Energy*, *34*(11), 2391-2398, (2009).

[19] Yeh, H. M., Ho, C. D., & Hou, J. Z., "The improvement of collector efficiency in solar air heaters by simultaneously air flow over and under the absorbing plate," *Energy*, *24*(10), 857-871, (1999).

[20] Yeh, H. M., Ho, C. D., & Hou, J. Z., "The improvement of collector efficiency in solar air heaters by simultaneously air flow over and under the absorbing plate," *Energy, 24*(10), 857-871, (1999).

[21] Jain, D., & Jain, R. K., "Performance evaluation of an inclined multi-pass solar air heater with in-built thermal storage on deep-bed drying application," *Journal of Food Engineering*, *65*(4), 497-509, (2004).

[22] Mohamad, A. A., "High efficiency solar air heater," *Solar Energy*, *60*(2), 71-76, (1997)

[23] Naphon, P., "Effect of porous media on the performance of the double-pass flat plate solar air heater," *International communications in heat and mass transfer*, *32*(1), 140-150, (2005).

[24] Bliss, R. W., "Solar House Heating–A Panel" In *Proceedings of the World Symposium on Applied Solar Energy*, (pp. 151-158), (1955).

[25] Swartman, R. K., & Ogunlade, O., "An investigation on packed-bed collectors," *Solar energy*, *10*(3), 106-110, (1996).

[26] Cheema, L.S., Mannan, D.K., Performance of parallel flow packed bed air heater," Silver Jubilee Congress, Atlanta, GA, 1, pp. 259- 263, (1979).

[27] Lansing, F. L., Clarke, V., & Reynolds, R., "A high performance porous flat-plate solar collector," *Energy*, *4*(4), 685-694, (1979).

[28] Collier, R. K., & Arnold, F. H., "Comparison of transpired beds for solar collector applications," *Proc. Annu. Meet.-Am. Sect. Int. Sol. Energy Soc.;(United States)*, *3*(CONF-800604-P2), (1980).

[29] Sorour M. M. & Hassab M. A., “a screen type solar air heater,” In Proc. Of the Eighth International Heat Transfer Conference 6, 3097-3103, (1986).

[30] Hassab M. A. & Sorour M. M., “Heat Transfer studies in matrix-type solar air heaters,” Journal of Solar Energy Engineering 111, 82-87, (1989).

[31] Kolb, A., Winter, E. R. F., & Viskanta, R., “Experimental studies on a solar air collector with metal matrix absorber,” *Solar Energy*, *65*(2), 91-98, (1999).

[32] Coppage, J. E., & London, A. L., “Heat transfer and flow friction characteristics of porous media,” Chem. Eng. Program (52), 57-56, (1956).

[33] Tong, L.S., London, A.L., “Heat transfer and flow friction characteristic of woven-screen and crosses-rod matrixes,” Trans ASME 79, 1558-1570, (1957).

[34] Kays, W.M., London, A.L., “Compact Heat Exchanger,” McGraw-Hill, New York, (1964).

[35] Hasatani, M., Itaya, Y., & Adachi, K., “Heat transfer and thermal storage characteristics of optically semi-transparent material packed bed solar heater, current researches in heat and mass transfer,” A Compendium and Festschrift for Prof. A. Ramachandram, ISHMT, Department of Mechanical Engineering, I.I.T., Madras, India, p. 61-70, (1985).

[36] Beckman, W. A., "Radiation and convection heat transfer in a porous bed," *Journal of Engineering for Power*, *90*, 51, (1968).

[37] Hamid, Y. H., Beckman, W. A., "Performance of air cooled radioactively heated screen matrices," J. Eng. Power 93, 221-224, (1971).

[38] Chiou, J. P., Ei-Wakil, M. M., "Heat transfer and flow friction characteristics of porous matrices with radiation as heat source," J. Heat Transf. 88, 69-76, (1966).

[39] Choudhary, C., Garg, H.P., "Performance of air heating collectors with packed air flow passage," *Solar Energy*, 50 (3), 205-221, (1993).

[40] Öztürk, H. H., & Demirel, Y., "Exergy-based performance analysis of packed-bed solar air heaters," *International journal of energy research*, *28*(5), 423-432, (2004).

[41] Sopian, K., Daud, W. R. W., Othman, M. Y., & Yatim, B., "Thermal performance of the double-pass solar collector with and without porous media," *Renewable Energy*, *18*(4), 557-564, (1999).

[42] Thakur, N. S., Saini, J. S., & Solanki, S. C. "Heat transfer and friction factor correlations for packed bed solar air heater for a low porosity system," *Solar Energy*, *74*(4), 319-329, (2003).

[43] Varshney L & Saini, J.S., (1998) Heat transfer and friction factor correlation for rectangular solar air heater duct packed with wire mesh screen matrices. Solar Energy 62 (4), 255-262, (1998).

[44] Mittal, M. K., & Varshney, L., "Optimal thermo-hydraulic performance of a wire mesh packed bed solar air heater," *Solar Energy 80,* 1112-1120, (2006).

[45] Ramadan, M. R. I., El-Sebaii, A. A., Aboul-Enein, S., & El-Bialy, E. "Thermal performance of a packed bed double-pass solar air heater.," *Energy*, *32*(8), 1524-1535, (2007).

[46] Choudhary, C., Garg, H.P., "Performance of air heating collectors with packed air flow passage," *Solar Energy*, 50 (3), 205-221, (1993).

[47] Sopian, K., Daud, W. R. W., Othman, M. Y., & Yatim, B., "Thermal performance of the double-pass solar collector with and without porous media," *Renewable Energy*, *18*(4), 557-564, (1999).

[48] Thakur, N. S., Saini, J. S., & Solanki, S. C. "Heat transfer and friction factor correlations for packed bed solar air heater for a low porosity system," *Solar Energy*, *74*(4), 319-329, (2003).

[49] Öztürk, H. H., & Demirel, Y., "Exergy-based performance analysis of packed-bed solar air heaters," *International journal of energy research*, *28*(5), 423-432, (2004). [48] http://www.omega.com/pptst/HHF42.html.

[50] Mittal, M. K., & Varshney, L., "Optimal thermo-hydraulic performance of a wire mesh packed bed solar air heater," *Solar Energy 80*, 1112-1120, (2006).

[51] Prasad, S. B., Saini, J. S., & Singh, K. M., "Investigation of heat transfer and friction characteristics of packed bed solar air heater using wire mesh as packing material," *Solar Energy*, *83*(5), 773-783, (2009).

[52] Produced for the U.S. Department of Energy (DOE) by the National Renewable Energy Laboratory, a DOE national laboratory DOE/GO-10098- 528, April 1998.

[53] David Ryan Ashley, thesis title 'Reducing ventilation energy demand in multifamily high rise buildings through preconditioning', Cornell University, May 2007.

[54] Matuszewski, P & Sawicka, M., thesis title "OPTIMIZATION OF SOLAR AIR COLLECTOR," Aalborg University, 2010, http://projekter.aau.dk/projekter/files/33024875/Master%20thesis%20-%20solar%20air%20collector.pdf, (Accessed on April 22, 2013).

[55] Omega, http://www.omega.com/pptst/HHF42.html, (Accessed on June 13, 2013).

[56] "Wheatstone Bridge," http://physics.kenyon.edu/EarlyApparatus/Electrical_Measurements/Wheatstone_Bridge/Wheatstone_Bridge.html, (Accessed on July 12, 2013)

[57] "Wheatstone Bridge," *DocStoc*, http://www.docstoc.com/docs/124541080/Wheatstone-Bridge---PowerPoint, (Accessed on July 17, 2013).

[58] THOMASENTNEWS,http://news.thomasnet.com/companystory/Economical-Hot-Wire-Anemometer-Series-HHF42-823026, (Accessed May 12, 2013).

[59] Karakoy Depo, http://www.karakoydepo.com/OBR-200M-2K-TEK-EMISLI-SALYANGOZ-FAN,PR-185.html, (Accessed on June 12, 2013).

[60] Ibid.

[61] Danial S., thesis title, "Solar Matrix Air Heater System," Eastern Mediterranean University, p. 21, August 2010.

[62] Department of Physics, National Tsing Hua University, http://www.phys.nthu.edu.tw/~gplab/file/Common%20equipment/Xplorer%20GLX_PS-2002%28Manual%29.pdf, (Accessed on June 17, 2013).

[63]XplorerGLX,http://www.emu.dk/gsk/fag/fys/dataopsamling/hvordan_kommer_man_videre/, (Accessed on June 19, 2013).

[64] Aldabbagh, L. B. Y., Egelioglu F., and Kawajah. M. F., "7th International Conference on Heat Transfer, Fluid Mechanics and Thermodynamics", Antalya, Turkey, (19-21, July 2010).

[65] Ibid

[66]"Data Normalization and Standardization," http://www.benetzkorn.com/wp-content/uploads/2011/11/Data-Normalization-and-Standardization.pdf, (Accessed on July 24, 2013).

[67] Aldabbagh, L. B. Y., Egelioglu F., and Kawajah. M. F., "7th International Conference on Heat Transfer, Fluid Mechanics and Thermodynamics", Antalya, Turkey, (19-21, July 2010).

.

APPENCES

Appendix A: Solar air heaters collectors designs

Figure A1: Solar air heater collectors.

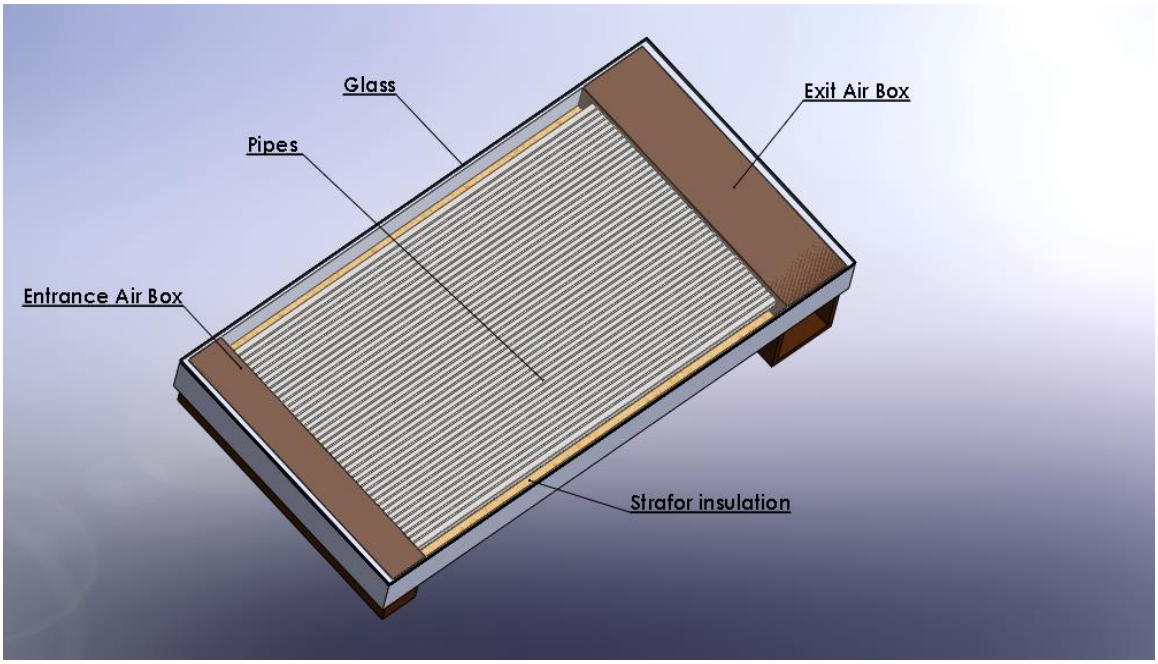

Figure A2: The design of the square aluminum tubes of the solar air heater collectors.

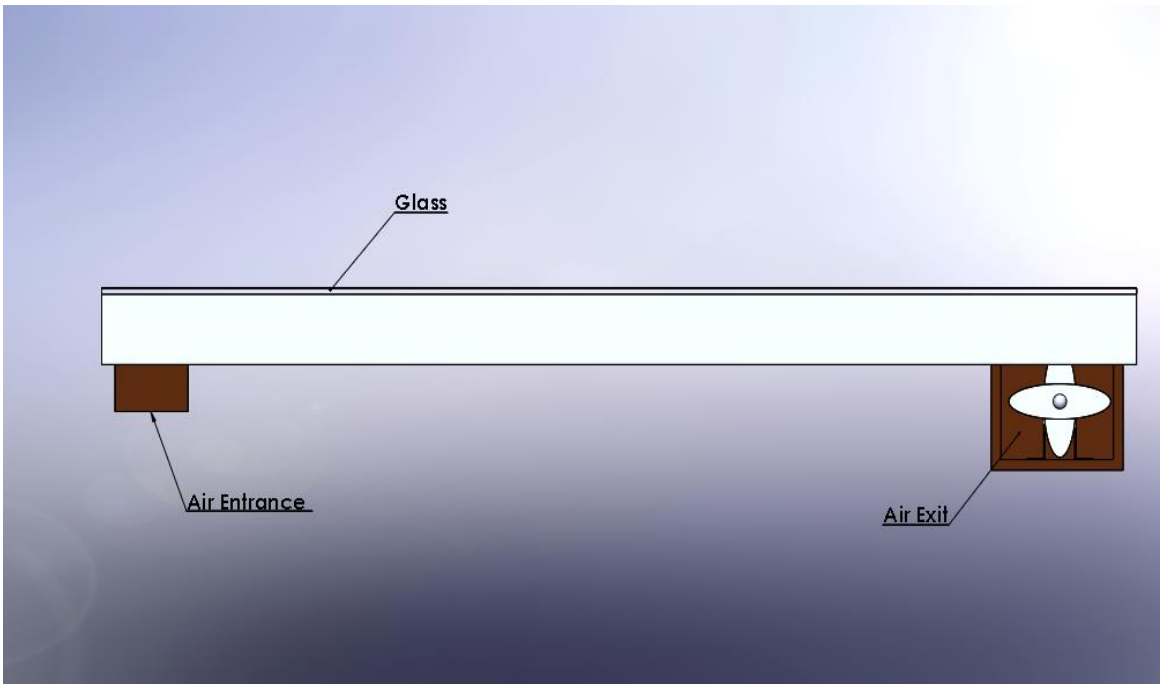

Figure A3: Side view of the panels.

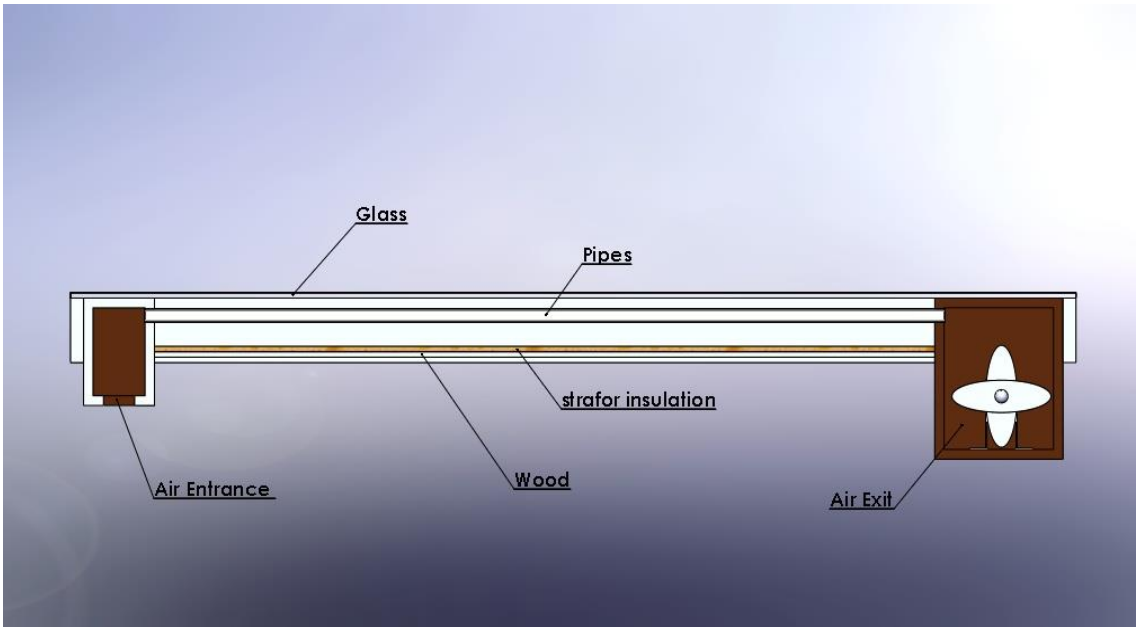

Figure A4: Side view of the panels and the instruments of the collectors.

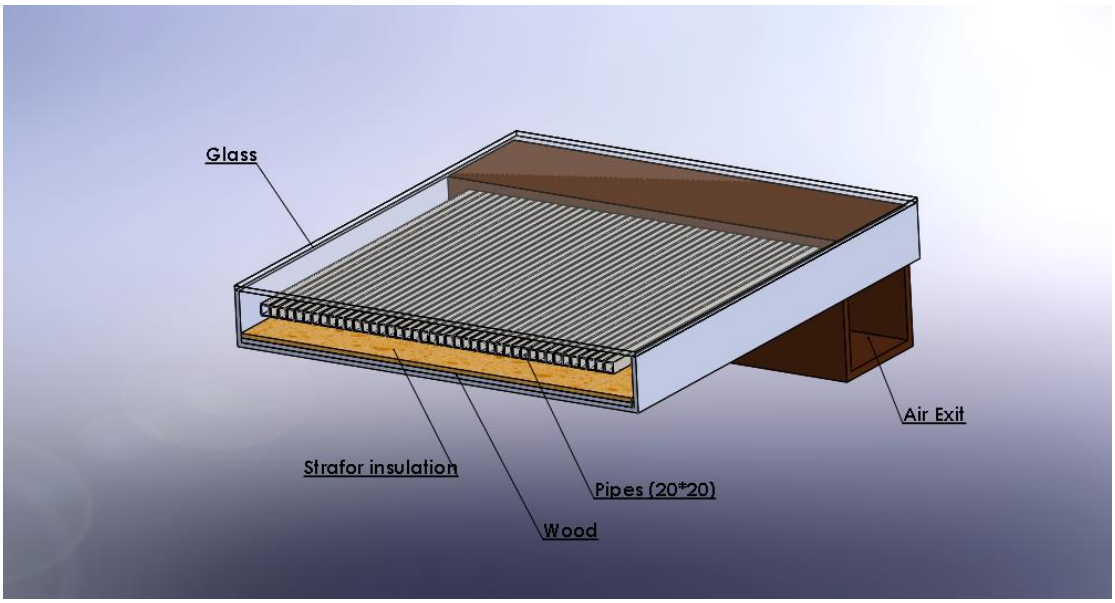

Figure A5: Sectional view of the (20 x 20 mm) Aluminum tubes.

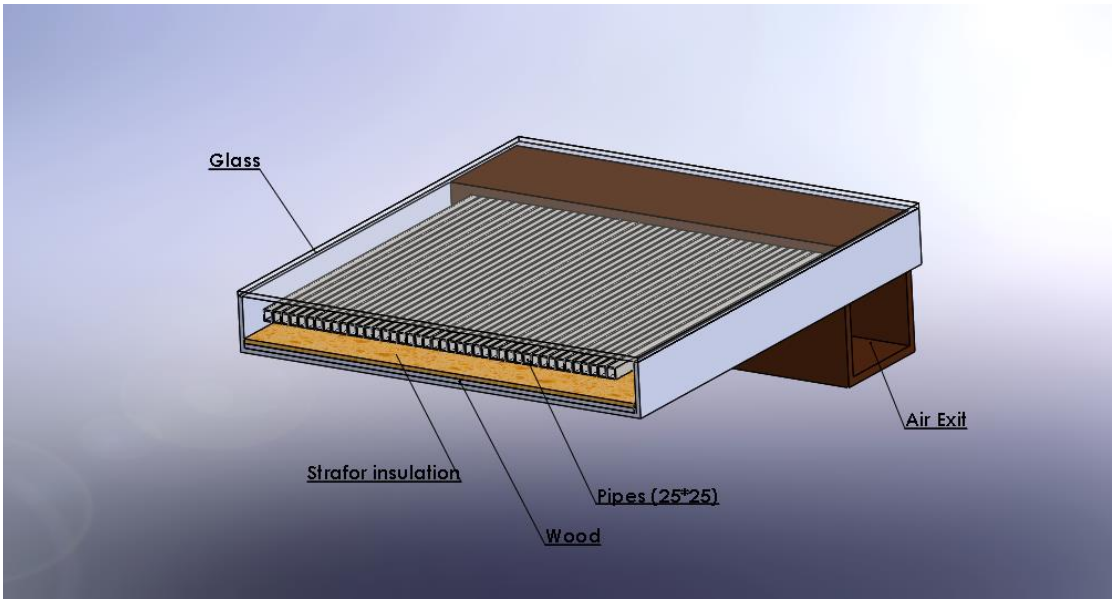

Figure A6: Sectional view of the (25 x 25 mm) Aluminum tubes.

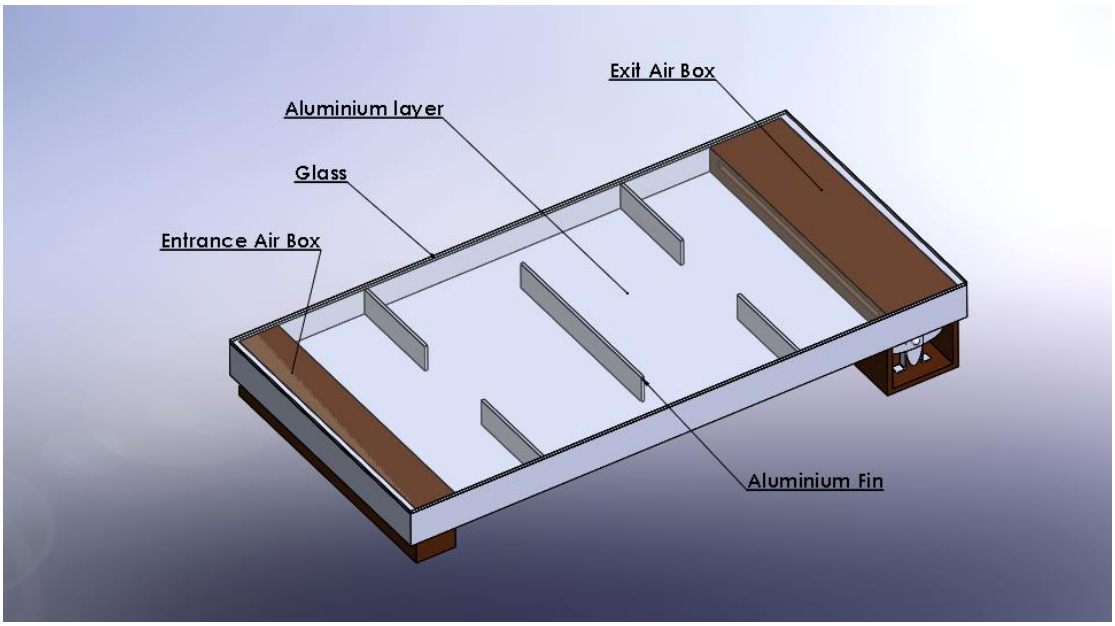

Figure A7: The design of fins' solar air heater collector.

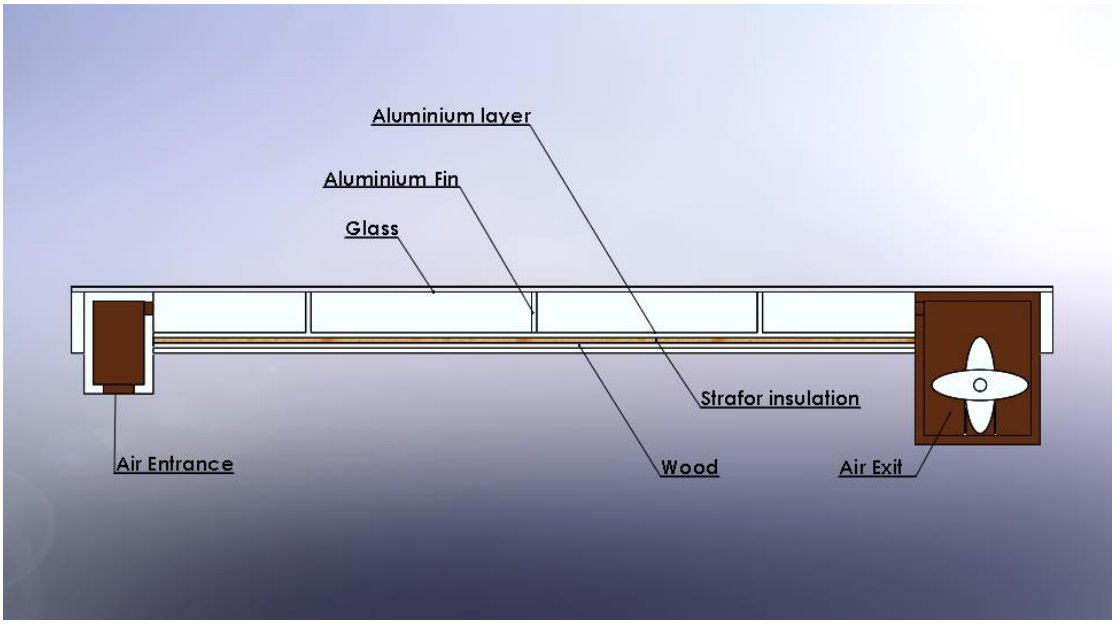

Figure A8: Side view of the fins collector.

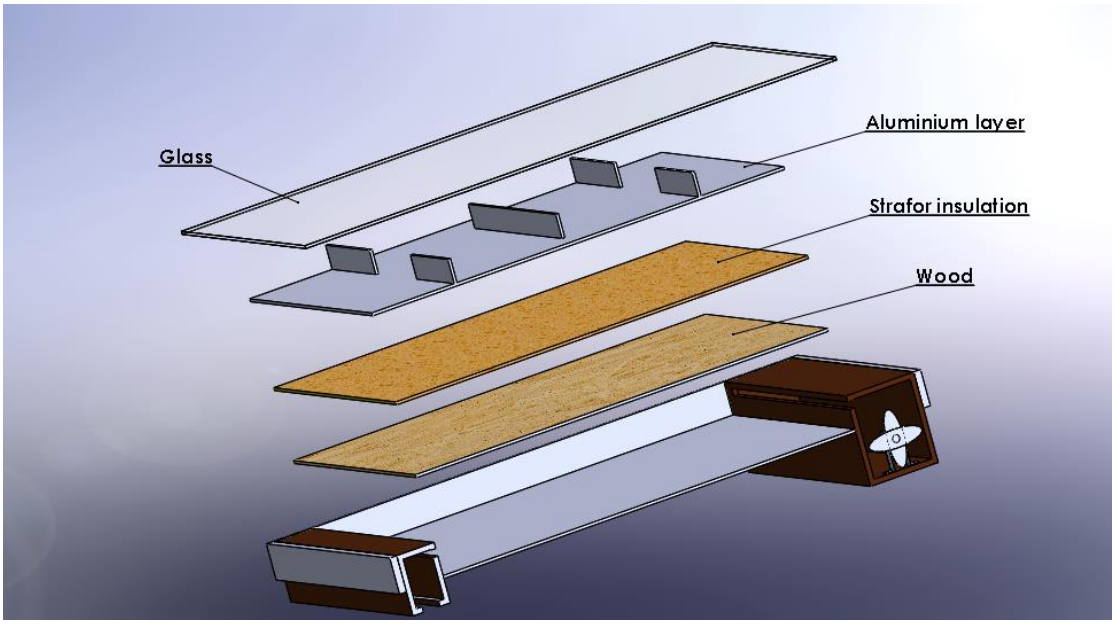

Figure A9: View of the parts of the fins' collector.

Appendix B: Normalization calculations

Fin type collector at (0.02kg/s)		
Time	ΔT	Fin type collector
08:00	8	0,10
09:00	12,8	0,33
10:00	19	0,63
11:00	25	0,91
12:00	26,8	1,00
13:00	26,3	0,98
14:00	24,8	0,90
15:00	21,6	0,75
16:00	17,8	0,57
17:00	11,7	0,27
18:00	6	0,00
Average=		0,58

(20 x 20 mm) tubes type collector at (0.02kg/s)		
Time	ΔT	(20 x 20 mm) Tubes type collector
08:00	7,8	0,04
09:00	12,6	0,26
10:00	19,6	0,57
11:00	26	0,85
12:00	29,1	0,99
13:00	29,4	1,00
14:00	28,2	0,95
15:00	25,1	0,81
16:00	20,7	0,62
17:00	13,5	0,30
18:00	6,8	0,00
Average=		0,58

previous study collector at (0.02kg/s)		
Time	ΔT	steel wire mesh layers collector
08:00	4	0,05
09:00	8,9	0,28
10:00	13,9	0,52
11:00	18,6	0,74
12:00	22,5	0,93
13:00	24	1,00
14:00	22	0,90
15:00	14,5	0,55
16:00	8	0,24
17:00	4,2	0,06
18:00	3	0,00
Average=		0,48

(25 x 25 mm) tubes type collector at (0.02kg/s)		
Time	ΔT	(25 x 25 mm) Tubes type collector
08:00	7,6	0,04
09:00	12	0,23
10:00	19,3	0,55
11:00	25,4	0,82
12:00	29,5	1,00
13:00	28,8	0,97
14:00	27,6	0,92
15:00	24,6	0,79
16:00	20,2	0,59
17:00	13,1	0,28
18:00	6,7	0,00
Average=		0,56

Figure B1: Temperature data normalization at 0.02 kg/s.

Fin type collector at (0.03kg/s)		
Time	ΔT	Fin type collector
08:00	6,7	0,09
09:00	11,7	0,37
10:00	15,2	0,57
11:00	19,7	0,82
12:00	22,5	0,97
13:00	23	1,00
14:00	22	0,94
15:00	19,4	0,80
16:00	16	0,61
17:00	9,7	0,26
18:00	5	0,00
Average=		0,59

(20 x 20 mm) tubes type collector at (0.03kg/s)		
Time	ΔT	(20 x 20 mm) Tubes type collector
08:00	7	0,09
09:00	12,3	0,36
10:00	15,9	0,55
11:00	20,7	0,79
12:00	23,5	0,94
13:00	24,7	1,00
14:00	22,7	0,90
15:00	20,5	0,78
16:00	16,8	0,59
17:00	10,5	0,27
18:00	5,3	0,00
Average=		0,57

previous study collector at (0.03kg/s)		
Time	ΔT	steel wire mesh layers collector
08:00	3,2	0,01
09:00	5,8	0,15
10:00	11,1	0,43
11:00	15,2	0,64
12:00	19,1	0,85
13:00	22	1,00
14:00	14,2	0,59
15:00	14,5	0,61
16:00	12	0,47
17:00	6,3	0,17
18:00	3	0,00
Average=		0,45

(25 x 25 mm) tubes type collector at (0.03kg/s)		
Time	ΔT	(25 x 25 mm) Tubes type collector
08:00	6,3	0,06
09:00	11,9	0,36
10:00	15,6	0,56
11:00	20,2	0,80
12:00	22,7	0,94
13:00	23,9	1,00
14:00	21,9	0,89
15:00	20	0,79
16:00	16,3	0,60
17:00	10	0,26
18:00	5,1	0,00
Average=		0,57

Figure B2: Temperature data normalization at 0.03 kg/s.

Fin type collector at (0.04kg/s)		
Time	ΔT	Fin type collector
08:00	4,4	0,02
09:00	9,2	0,30
10:00	14	0,59
11:00	18,1	0,83
12:00	19,6	0,92
13:00	21	1,00
14:00	18,7	0,86
15:00	16,5	0,73
16:00	13,5	0,56
17:00	9,1	0,30
18:00	4,1	0,00
Average=		0,55

(20 x 20 mm) tubes type collector at (0.04kg/s)		
Time	ΔT	(20 x 20 mm) Tubes type collector
08:00	7,8	0,04
09:00	12,6	0,26
10:00	19,6	0,57
11:00	26	0,85
12:00	29,1	0,99
13:00	29,4	1,00
14:00	28,2	0,95
15:00	25,1	0,81
16:00	20,7	0,62
17:00	13,5	0,30
18:00	6,8	0,00
Average=		0,58

previous study collector at (0.04kg/s)		
Time	ΔT	steel wire mesh layers collector
08:00	2,8	0,02
09:00	5,7	0,20
10:00	10,5	0,50
11:00	15,9	0,84
12:00	16	0,84
13:00	18,5	1,00
14:00	14,5	0,75
15:00	12,2	0,61
16:00	8	0,34
17:00	3	0,03
18:00	2,5	0,00
Average=		0,47

(25 x 25 mm) tubes type collector at (0.04kg/s)		
Time	ΔT	(25 x 25 mm) Tubes type collector
08:00	4,5	0,01
09:00	9,6	0,30
10:00	14,8	0,60
11:00	18,6	0,81
12:00	21,5	0,98
13:00	21,9	1,00
14:00	19,6	0,87
15:00	17,7	0,76
16:00	15,2	0,62
17:00	10	0,32
18:00	4,3	0,00
Average=		0,57

Figure B3: Temperature data normalization at 0.04 kg/s.